NASA Conference Publication 2451

Joint University Program for Air Transportation Research—1983

Proceedings of a conference held in Atlantic City, New Jersey December 16, 1983

NASA

NASA Conference Publication 2451

Joint University Program for Air Transportation Research—1983

Compiled by
Frederick R. Morrell
Langley Research Center
Hampton, Virginia

Proceedings of a conference sponsored by the National Aeronautics and Space Administration and the Federal Aviation Administration and held in Atlantic City, New Jersey
December 16, 1983

National Aeronautics and Space Administration

Scientific and Technical Information Branch

1987

PREFACE

The Joint University Program for Air Transportation Research is a coordinated set of three grants jointly sponsored by NASA Langley Research Center and the Federal Aviation Administration, one each with Massachusetts Institute of Technology (NGL-22-009-640), Ohio University (NGR-36-009-017), and Princeton University (NGL-31-001-252), to support the training of students for the air transportation system. These grants, initiated in 1971, encourage the development of innovative curriculums and support the establishment of graduate and undergraduate research assistantships and internships.

An important feature of this program is the quarterly review, one held at each of the schools and a fourth at a NASA or FAA facility. This latter review for 1983 was held at the Federal Aviation Administration Technical Center, Atlantic City, New Jersey, December 16, 1983. At these reviews the program participants, both graduate and undergraduate, have an opportunity to present their research activities to their peers, professors, and invited guests from government and industry.

This conference publication represents the fourth in a series of yearly summaries of the activities of the program (the 1982 summary appears in NASA CP-2285). The majority of the material is the effort of the students supported by the grants.

Three types of contributions are included. Completed works are represented by full technical papers. Research previously in the open literature (for example, theses or journal articles) is presented in an annotated bibliography. Status reports of ongoing research are represented by copies of viewgraphs augmented with a brief descriptive text.

Use of trade names or manufacturers in this report does not constitute an official endorsement of such products or manufacturers, either expressed or implied, by the National Aeronautics and Space Administration or the Federal Aviation Administration.

Frederick R. Morrell
NASA Langley Research Center

CONTENTS

MASSACHUSETTS INSTITUTE OF TECHNOLOGY

INVESTIGATION OF AIR TRANSPORT TECHNOLOGY AT MASSACHUSETTS INSTITUTE OF TECHNOLOGY, 1983

Robert W. Simpson
Director, Flight Transportation Laboratory
Massachusetts Institute of Technology
Cambridge, Massachusetts

SUMMARY OF RESEARCH

Runway Approach Guidance Using Loran-C

1.0 Introduction

For 1983, research activity in the NASA Joint University Program for Air Transportation Technology has concentrated on several topics connected with investigating the use of Loran-C for flying "pseudo-precision" approaches to runways at low density general aviation airports. These topics have arisen in preparation for a flight test demonstration of approaches to be flown at Hanscom airport in Bedford, Mass. The goal of this research has evolved to determining the limitations in providing both centerline and altitude guidance for runways in good Loran-C signal coverage. The high data rate (10 per second) and good "repeatable" accuracy (60 feet, 1σ) of Loran-C indicate that it will be possible to provide the pilot with a continuous, cross pointer display of guidance information similar to that provided by ILS/MLS, at least when good signal-noise ratios and good geometry from Loran-C LOP's (Lines of Position) exist at the airport.

The research goals are to demonstrate approach guidance of higher quality than prior demonstrations of where L-NAV approaches to the airport in the direction of the runway have been flown. The intention here is to provide performance more similar to ILS/MLS, and to determine the degradation of guidance performance as geometrical and signal-noise factors degrade. With the advent of very low cost, high performance Loran-C receivers for general aviation to approach guidance for use in enroute area-navigation, it is timely to explore this application, since the results may have pertinence to decisions on deploying MLS/ILS in the NAS (National Airspace System) and the future role of GPS (Global Positioning System) for general aviation.

2.0 Description of the Concept

The basis for the concept lies in the remarkable stability of points located in Loran-C TD (Time Difference) coordinates over extended periods of time. Prior work by students in this program (see ref. 1) noted that the repeatable accuracy over long periods of time was a few hundred feet, and over a short duration perhaps 60 feet. This leads one to try to use this short term repeatable accuracy and the high position rate of Loran-C by establishing a local tangent plane coordinate frame, centered on the touchdown point. The location of the origin of this coordinate frame can be described in Loran-C TD values which are published and perhaps updated by the pilot at the time of initiating the Loran-C approach. A simpler conversion of Loran TD's can be made into the local tangent plane coordinate frame at high data rates, and is independent of the errors in modelling the Earth's reference ellipsoid and variations in signal propagation velocity, thereby avoiding some of the major sources of Loran-C error for enroute flying.

The Loran-C receiver can provide data at a rate of roughly 10 times per second on cross-track and along-track position and position rate. This can be suitably filtered, and combined with heading rate data in a microprocessor before generating signals for the autopilot or pilot display. Since distance to touchdown is known, the nominal glide slope altitude can be determined very accurately. This can be displayed separately, or combined with signals from an encoding altimeter to display the current altitude deviation to the pilot. Both cross-track and altitude deviation signals can be displayed electronically.

3.0 The Loran-C Approach Guidance Display

A special display has been designed and constructed which uses a microprocessor to interpret data from the Loran-C receiver and drive bar-graph and seven-segment LED's display units. The Loran-C receiver (Micrologic ML-3000) has been especially modified to transmit filtered data on TD and TD rate once per second via a RS232 link, and the filter constants of the receiver can be set by the experimenter.

Figure 1 shows the current layout of the front panel of the Loran-C Approach Guidance Display in its present configuration. The top bar-graph LED display will show right-left cross track deviations from the runway centerline. The bottom LED will be used to show cross-track velocity. The seven-segment LED displays on the right side of the display will give numerical readout of range to touchdown and glide slope altitude. The microprocessor program for the display has been written and tested for a current version which uses only Loran-C data. Later developments will accommodate data from heading rate gyros and the encoding altimeter, and display glide path deviation.

There are several alternate display options which have been considered. The original P-POD CRT display developed under this grant was abandoned in favor of the new display of figure 1. A digitally driven, electro-mechanical round display has also been constructed and will be flown to test its operation. In January 1983, Norry Dogan, an undergraduate at MIT, visited Langley Research Center for 1 week to work with Langley personnel on constructing the display of figure 1.

During that week, a display case was built, printed circuit boards were designed by Langley personnel from a pin diagram of the display circuit supplied by MIT, and some software problems were solved. The printed boards were subsequently manufactured at Langley Research Center. They replace the wire wrapped board built at MIT.

Finally, a flat panel, bit mapped LCD display (3-1/2" by 7") has been purchased for general experimentation; it was planned in the next year's work to develop digital circuitry to create an approach display using this device for the next year's work.

4.0 The Fluidic Rate Gyro and Encoding Altimeter

A fluidic rate gyro originally conceived at NASA Langley Research Center has been developed further at MIT. Further modifications are planned to improve its frequency response before incorporating it in the approach guidance system. The original thermistors were modified to keep them at a constant temperature, and now they are being replaced with hot-wire elements with less thermal inertia.

As a result of a conversation between John Einhorn, another undergraduate at MIT, and Mr. Gary Burrell, Vice President Engineering, King Radio Corp. at the June 1983 Research Progress meeting at Ohio University, MIT received a Model 5035 electrical encoding altimeter. It was to be incorporated into the approach guidance system by Einhorn in the next year.

5.0 Ground Survey of Loran-C Signals at Hanscom Field

In the period November 1983 - January 1984 the ML-3000 receiver was mounted in ground vehicles for various preliminary tests of its operations. Data were displayed and stored using an Apple II computer, and later printed out. These tests showed the short term accuracies of the receiver, and its transient response to speed changes of the ground vehicle. Typical data obtained are shown in figures 2, 3, 4, and 5 where the filter constants for a slow moving vehicle (marine) and fast moving vehicle (aircraft) are being used.

Figures 2 and 3 show the transient response of position data to accelerating the vehicle to a given speed, and then decelerating to a stop for the two filters. Figures 4 and 5 provide some data on the effect of poor SNR (Signal Noise Ratio) on the standard deviation of short term position data while stationary. Notice that the aircraft position data degrades from 0.07 μsec (69 feet) at good SNR to values around 0.2 μsec (196 feet) when SNR is -20 dB. If the ship filter constants are used, the heavy slow filter greatly improves these short term standard deviations to values of 0.02 μsec (20 feet) at good SNR and 0.08 μsec (80 feet) at poor SNR. Further experimentation is planned on these data which will include information on TD rates output by the receiver. The data gathering programs have been written for the Apple Computer, including a Fast Fourier Transform coding which will provide information on the spectral distribution of those error signals.

In January, a preliminary ground survey of the Loran-C signal grid around Hanscom field was carried out to discover any anomalies, and to measure the TD gradients from the Caribou-Seneca and Nantucket-Seneca LOP's. Touchdown points for all runways were surveyed, as well as a variety of points around the periphery of the airport. Figure 6 shows the location of the test points around the airfield, as well as the Loran-measured position. The Airport Reference Point was chosen as the Loran reference point, and its TD's adjusted to obtain a zero mean error for all 21 points surveyed. From these data, it was discovered that anomalies of several hundred feet could exist at hangars, amongst trees, and on sloping ground. This suggests more effort be expended in surveying the airport, and that a balloon platform should be constructed to raise the Loran-C antenna off the ground surface to see if these surface anomalies disappear, and to explore the final approach airspace along the glide slope.

In general, a good Loran-C grid exists at Hanscom field, and the measured and calculated TD gradients show excellent agreement. For Seneca-Caribou, the measured gradient was 161.5 m/μsec, compared to the theoretical (v = 1) 162.6 m/μsec for Hanscom. For Seneca-Nantucket, the measured gradient was 177.5 m/μsec compared to the theoretical 180.4. Since the 99% confidence interval for the sample is ±6 m/μsec, this difference is not statistically significant. These survey points are to be extended (fig. 6).

6.0 Computer Simulation of Loran-C Approach Flying

Finally, a computer simulation of approach flights to Hanscom has been initiated to allow more detailed exploration of the effects of all these parameters on expected approach guidance. With the knowledge of the signal geometry, the statistical Loran data output by the receiver over space and time, it will be possible to explore the effects of crosswind, the mixing of heading rate and altitude signals, etc., and to repeat many simulated approaches to see the average statistical performance of the guidance system and display.

Reference

1. Natarajan, K., Use of Loran C for General Aviation Aircraft Navigation, 2/1981, MIT Flight Transportation Laboratory (FTL) Report 81-2.

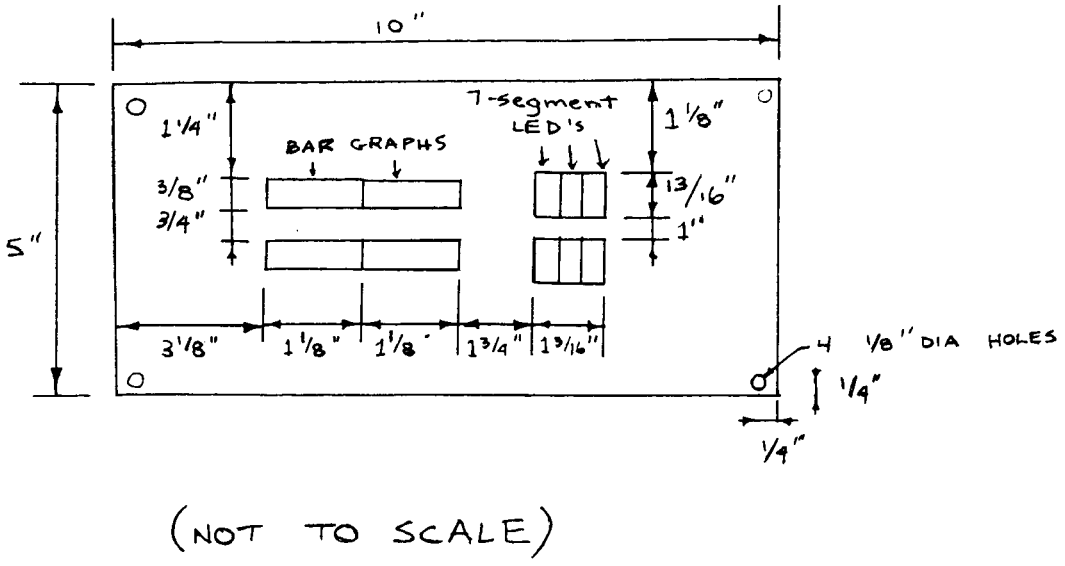

(NOT TO SCALE)

Figure 1. Loran-C approach guidance display.

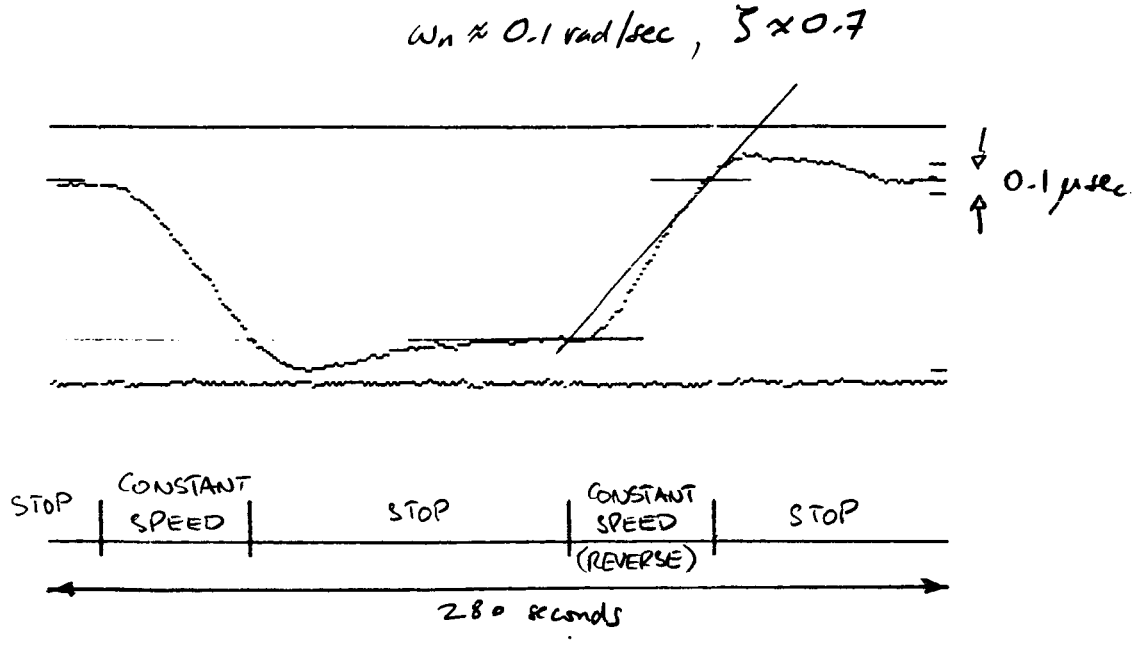

Figure 2. Transient response of marine filter.

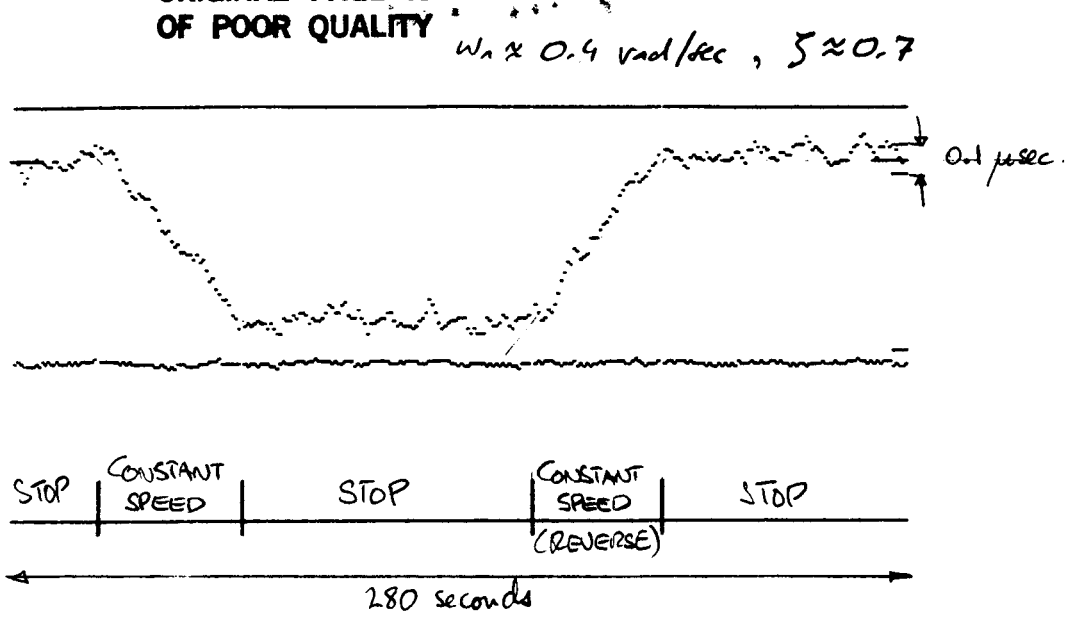

Figure 3. Transient response of aircraft filter.

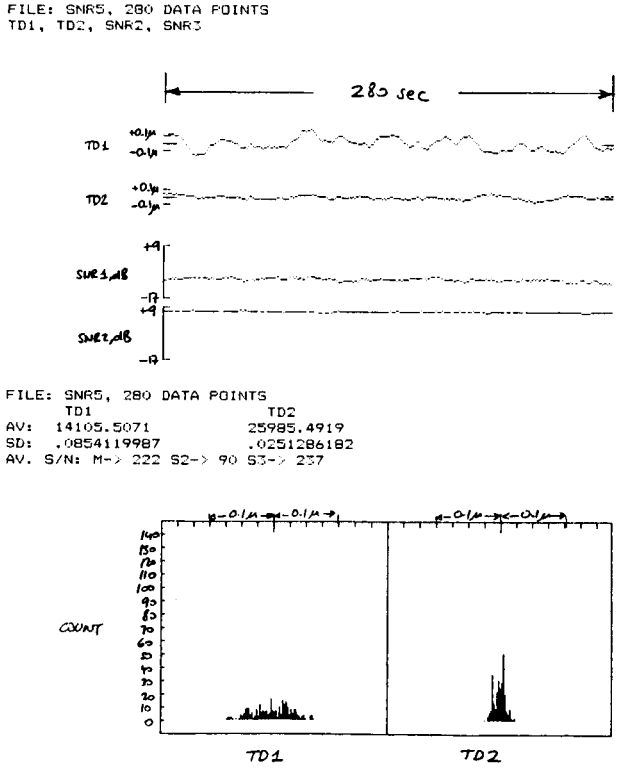

Figure 4. Effect of SNR on short-term TD variation.

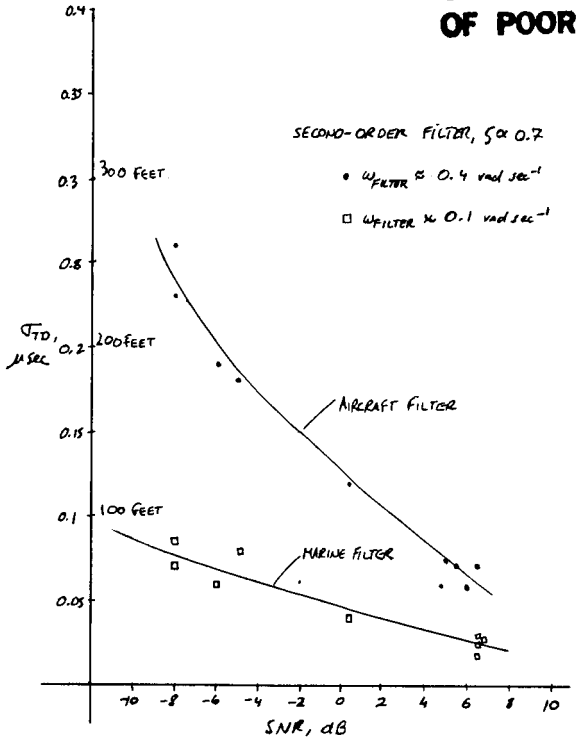

Figure 5. Short-term variation in position versus SNR.

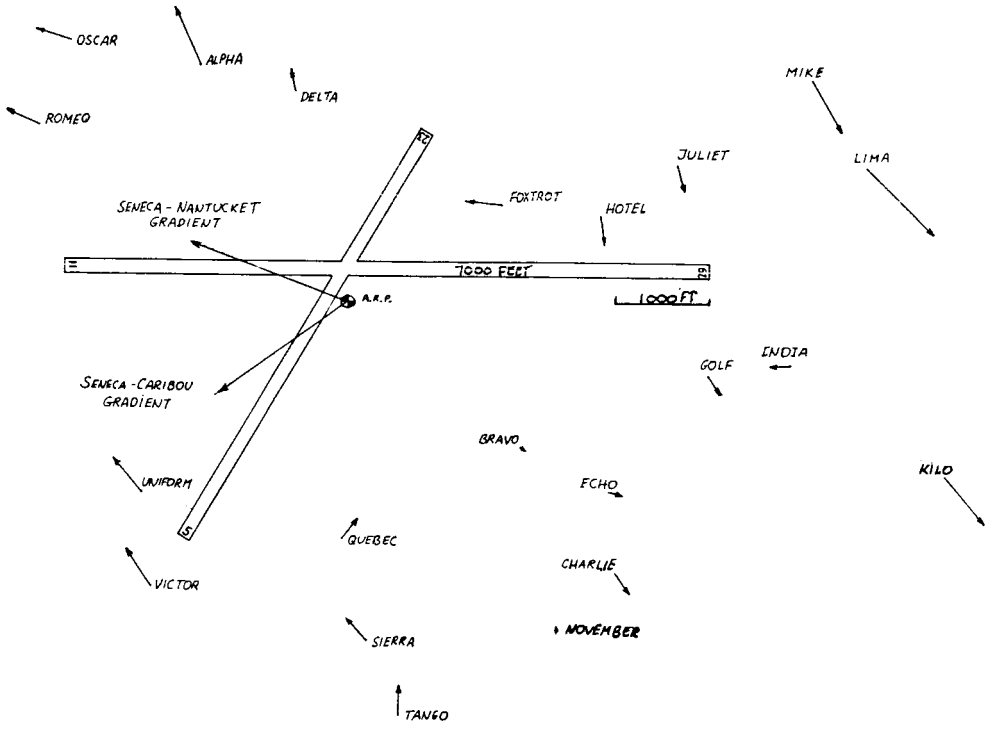

Figure 6. Loran-C survey at Hanscom Field, residual errors in touchdown position.

DEVELOPMENT OF AN LED DISPLAY SYSTEM FOR CROSS-TRACK DISTANCE AND VELOCITY FOR LORAN-C FLIGHT

Norry Dogan
Flight Transportation Laboratory
Massachusetts Institute of Technology
Cambridge, Massachusetts

Abstract

Figure 1 illustrates in block diagram the methodology for estimating cross-track velocity by combining rate-gyro and Loran-C data. At present preliminary analysis has established values for K_1, K_2, the parameters of the digital control loops.

A computer program has been written to implement a digital simulation of the system as illustrated in figure 2. Given a model for the noise in the rate-gyro and Loran-C receiver, and their dynamic response, the simulation provides a working model to establish good control loop parameters.

The layout of the LED display for flight testing of Loran-C approach flying, which was constructed during a visit to Langley Research Center, is shown in figure 3. Four bar-graph LED displays are paired to provide cross-track distance and velocity from a Loran-C defined runway centerline. Two seven-segment LED displays are used to provide alphanumeric readout of range to touchdown and desired height. A metal case was built, a circuit board designed, and manufactured with the assistance of NASA Langley personnel.

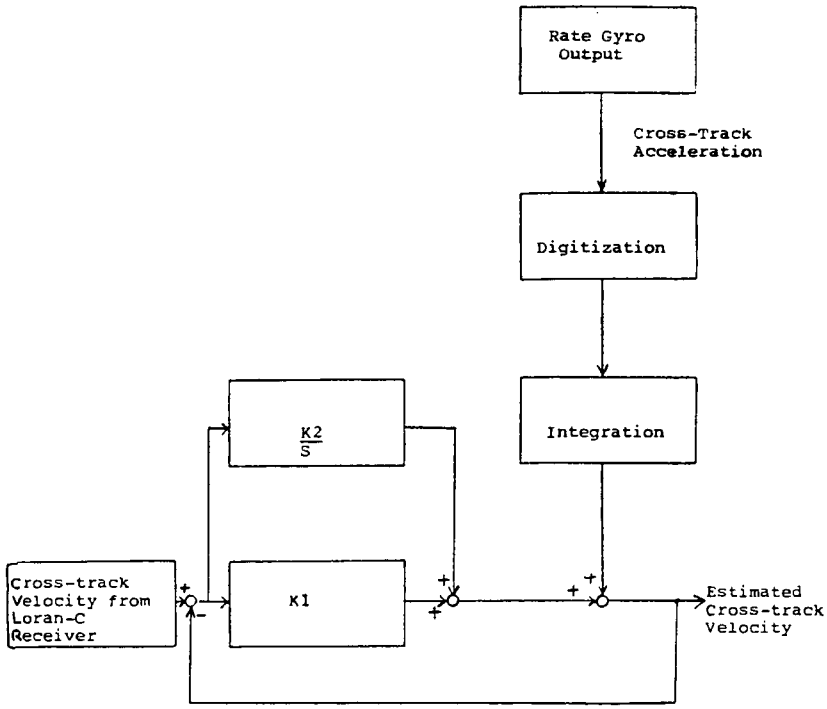

Figure 1. Block diagram - optimal estimation of cross-track velocity.

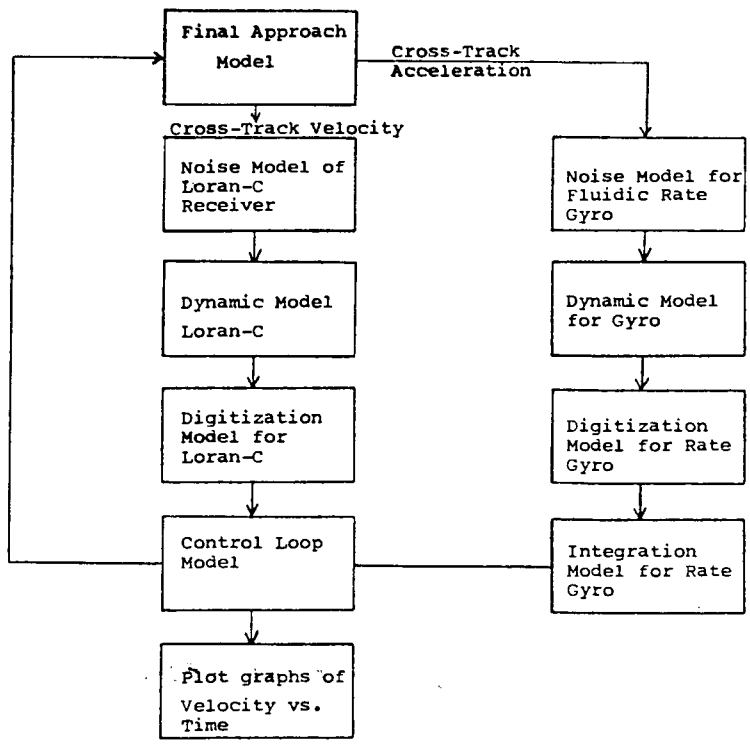

Figure 2. Digital simulation of the optimal cross-track velocity system.

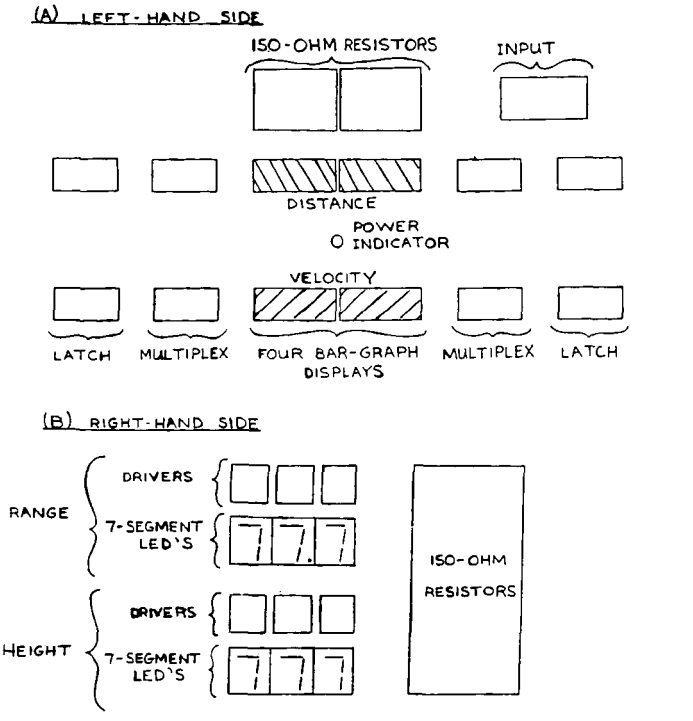

Figure 3. Layout of LED display for Loran-C flight.

LORAN-C APPROACH GUIDANCE PROJECT: CURRENT STATUS

A. L. Elias
Flight Transportation Laboratory
Massachusetts Institute of Technology
Cambridge, Massachusetts

Abstract

There are four areas of work in the Loran-C approach flight test project (fig. 1). Current results provide performance data on the effects of Signal Noise Ratio, SNR, on the dynamic performance of the receiver filters for Loran-C data, and data on Loran-C grid deformation at a microscale of 100 meters.

The Loran-C receiver provides an LOP (line of position) Master and Slave transmitter at an angle θ to magnetic north (fig. 2). No transformation to latitude-longitude reference frame is required since this is the major source of Loran-C navigation errors.

A local coordinate frame is established centered at touchdown point on the runway with directions along and across the runway (fig. 3). The coordinate transformation is shown as a simple pair of equations which can be easily computed.

A Loran-C data collection system has been set up as shown in figure 4. The Loran-C data are sent directly to an Apple II computer with a 12-inch monitor. The system has been installed in various ground vehicles with a 24-inch whip antenna mounted on the roof. This serves as a mobile platform for micro grid surveys and investigation of receiver dynamics.

The effect of SNR on Loran-C precision is shown for two receiver filters of different frequency response (fig. 5). The standard deviation of Loran-C is less than 0.1 microsecond (100 feet) at positive values for SNR.

A set of ground level static readings of touchdown (TD) was taken around Hanscom Field and transferred to an accurate detailed layout drawing; this showed local distortions of the average TD values as shown in figures 6 and 7. Similar surveys on a grid on the athletic fields at MIT showed variations over 100 meter spacing.

It is not clear why these microdistortions exist. They may not exist if the Loran-C antenna were a few hundred feet in the air, which suggests a 3-D survey in the approach area (fig. 8).

A possible method for a 3-D survey of micro grid distortions of Loran-C signals is shown. There are difficulties in locating a balloon precisely when winds exist, and a more mobile system to move over the micro grid is desired (fig. 9).

MAJOR AREAS:

- ALGORITHM DEVELOPMENT
- DISPLAYS AND PROCEDURES
- SENSOR BLENDING
- PERFORMANCE AND STANDARDS

PERFORMANCE - CURRENT TOPICS

- STATIC PERFORMANCE - EFFECT OF SNR
- DYNAMIC PERFORMANCE - FILTERS
- GRID MICRODEFORMATION

Figure 1. Loran-C approach nav - status.

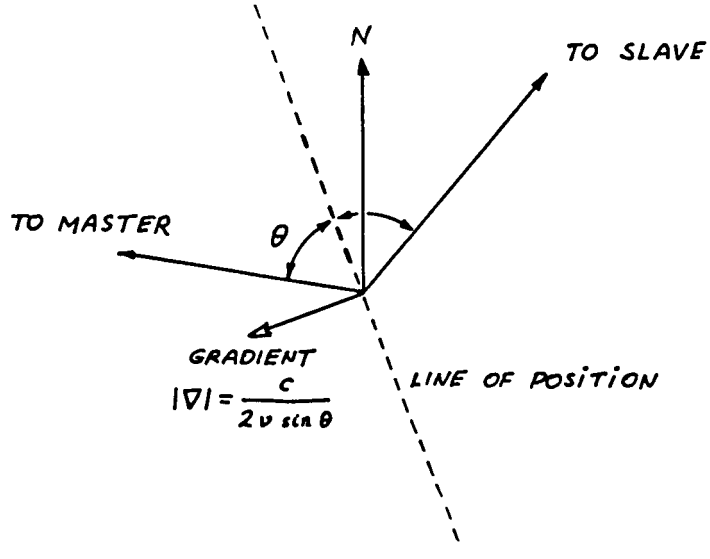

Figure 2. Local Loran geometry.

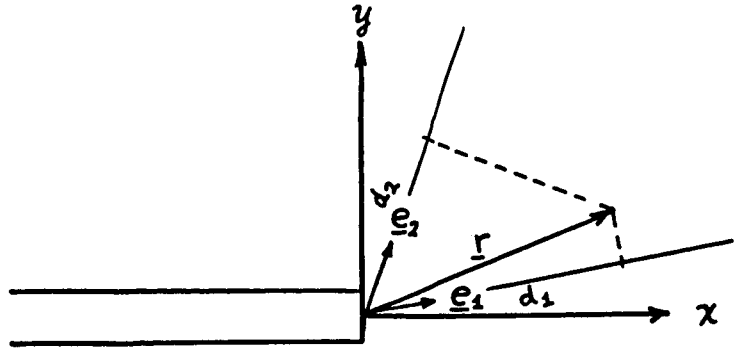

$$d_1 = \underline{r} \cdot \underline{e}_1 \quad d_2 = \underline{r} \cdot \underline{e}_2 \rightarrow \begin{Bmatrix} d_1 \\ d_2 \end{Bmatrix} = \begin{bmatrix} e_{1x} & e_{1y} \\ e_{2x} & e_{2y} \end{bmatrix} \begin{Bmatrix} r_x \\ r_y \end{Bmatrix}$$

$$\begin{Bmatrix} r_x \\ r_y \end{Bmatrix} = \begin{bmatrix} e_{1x} & e_{1y} \\ e_{2x} & e_{2y} \end{bmatrix}^{-1} \begin{Bmatrix} d_1 \\ d_2 \end{Bmatrix}$$

Figure 3. Coordinate transformation.

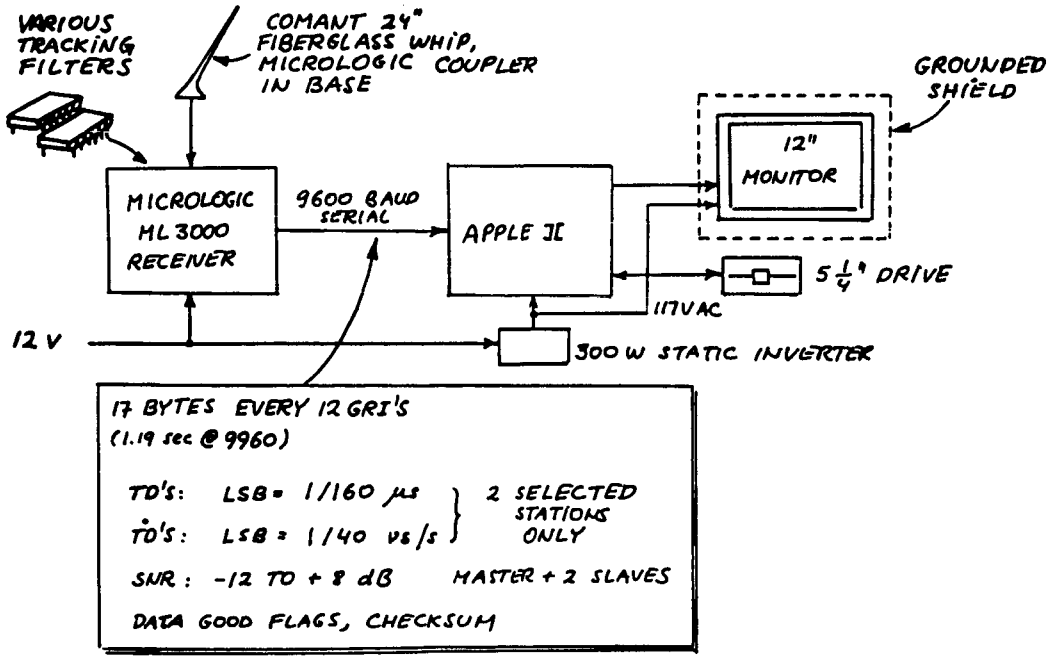

Figure 4. Loran-C data collection setup.

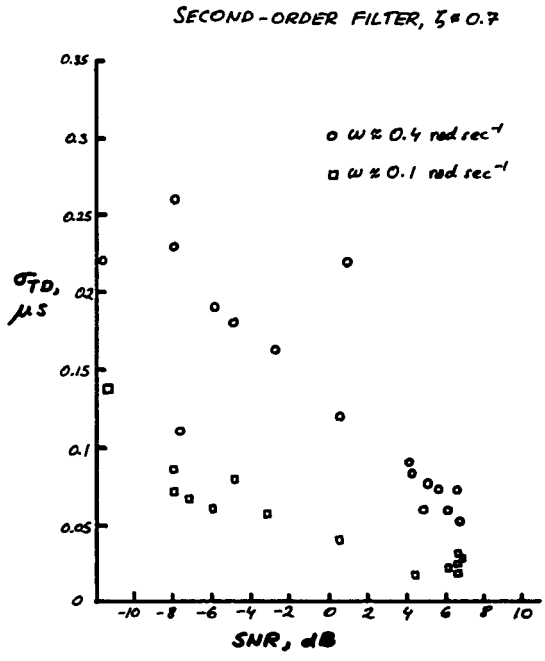

Figure 5. Short-term variation in TD.

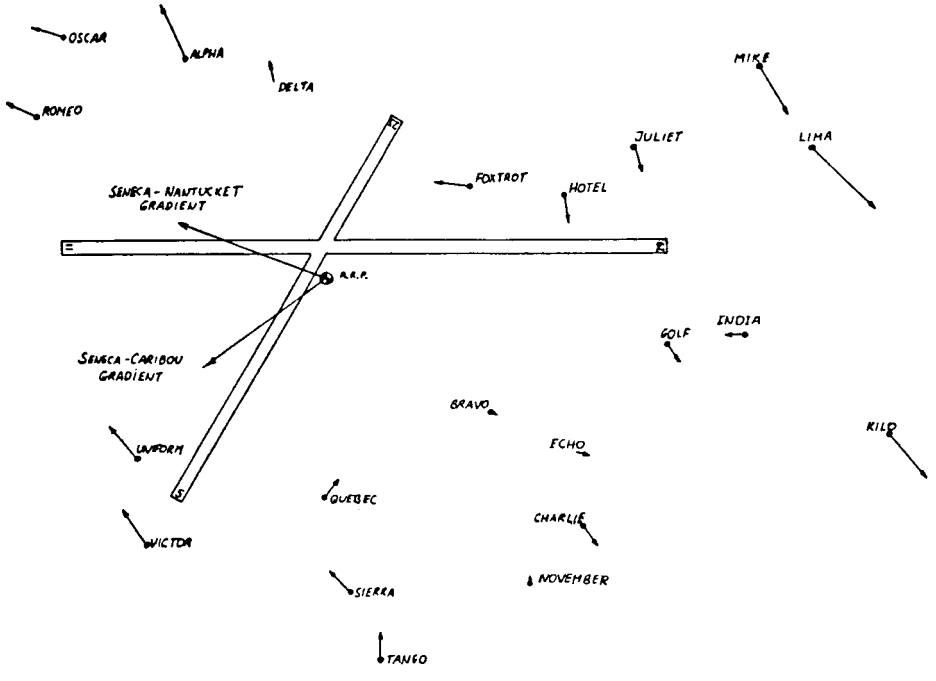

Figure 6. Hanscom Field ground-level survey.

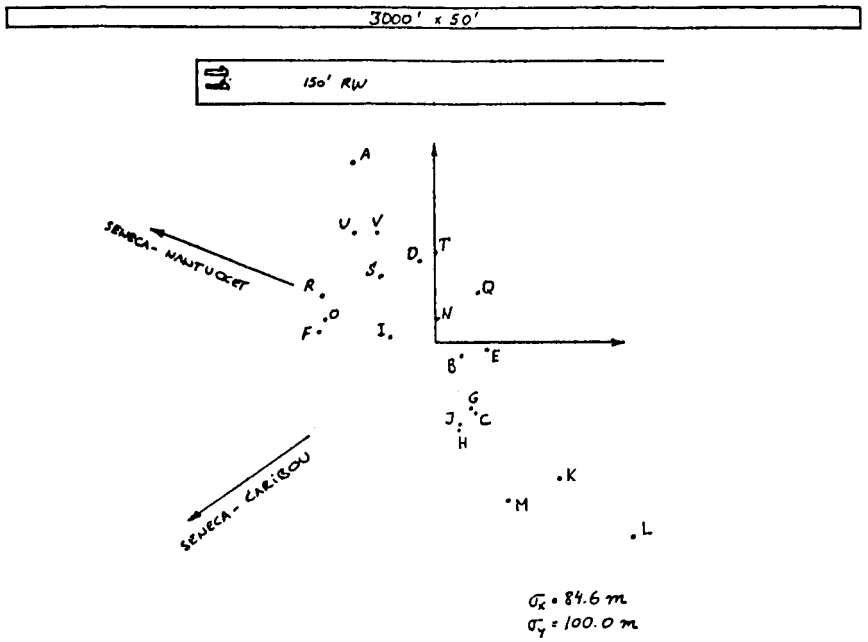

Figure 7. Summary of residual errors.

- EFFECT OF ANTENNA/VEHICLE ORIENTATION
- EFFECT OF SNR'S
- POSITION CORRELATION/CHARACTERISTIC LENGTH
- EFFECT AT ALTITUDE

NEED: DETAILED, POSSIBLY 3-D, SURVEY

Figure 8. Grid microdeformation - open items.

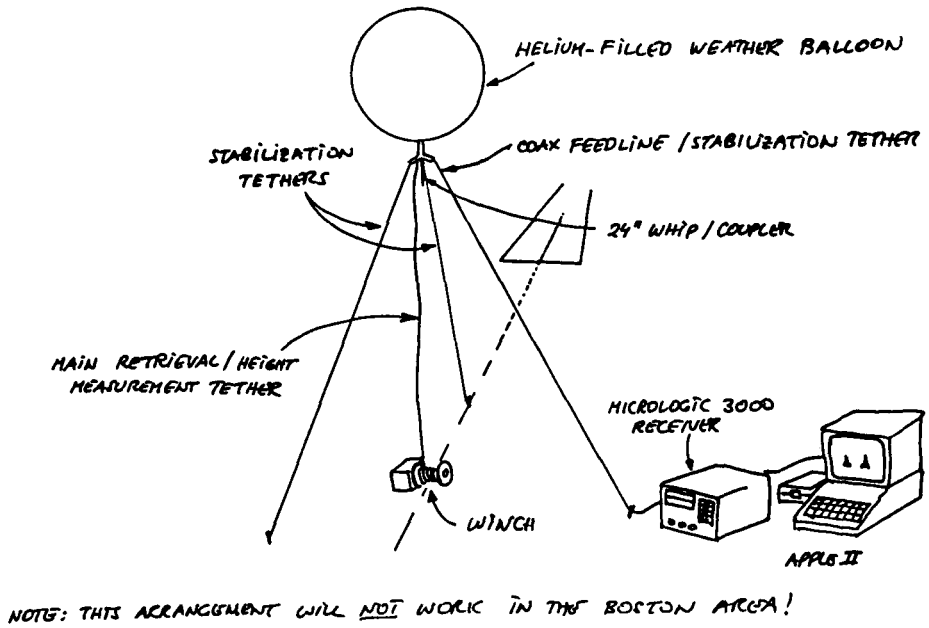

Figure 9. Balloon-borne antenna for 3-D survey.

OHIO UNIVERSITY

AIR TRANSPORTATION TECHNOLOGY PROGRAM

AT OHIO UNIVERSITY, 1983

Richard H. McFarland and
James D. Nickum
Avionics Engineering Center
Department of Electrical and Computer Engineering
Ohio University
Athens, Ohio

INTRODUCTORY REMARKS

The Air Transportation Technology Program at Ohio University, supported as a Joint-University Program effort by the National Aeronautics and Space Administration and the Federal Aviation Administration, dedicated the year 1983 principally to producing a specific research tool, viz, a flexible Loran-C receiver.

It was a successful year for the design and testing of the hardware. During 1983 several improvements to the Loran-C research receiver were made to allow this device to function more reliably and to provide a means to achieve flight test data with less difficulty.

Many of the changes to the receiver made in 1983 were natural extensions of the work completed in 1982 at Ohio University. The changes made involved a complete re-packaging of the receiver. The 1983 changes were to the performance and capability of this Loran-C receiver.

The ability to operate the receiver off of a single, simple power supply contained in the receiver was developed. This power supply consists of two switching DC to DC converters that provide + 5 VDC and ± 12VDC from an 8 to 40 VDC input supply system in the vehicle. The switching supplies are 75 to 85% efficient and therefore do not contribute significantly to power consumption of the receiver. Additionally, the complete power supply fits into a double wide slot in the receiver card-cage. This capability allows the entire receiver to be contained in a 19.5 inch rack panel that is only 5.25 inches tall and 9.0 inches deep.

The next change to the receiver that allowed a computation performance improvement was the new timing board design. This permitted a decrease in the time that the processor spent in wait loops. In the previous timing board design the processor had to wait for the digit strobes from the master timing chip to read each of the digits of the Loran-C pulse time. This wasted as much as 200 microseconds for each Loran-C pulse. This has been changed with the addition of hardware to produce an interrupt to the processor when the data from the timing chip is ready for output. Since there are 25 individual Loran-C pulses in the current 3 stations tracked and each pulse requires 5 digits to be read, a significant amount of time was wasted with the older timing board. The improvement with a 9960 GRI is greater than 25% per GRI.

Another hardware improvement involved the ability of the Loran-C receiver to treat all of the received Loran-C stations equally so that determination of the correct track point on the Loran-C pulse was achieved for stations of differing signal strengths. This was accomplished with a multiplexed sampled AGC system. This would allow increased accuracy in the determination of the correct tracking point on the Loran-C pulse. The hardware is complete and ready for integration into the current Loran-C receiver software.

The most significant improvement to the Loran-C receiver involved the implementation of Random Navigation capability (RNAV) in the O.U. Loran-C receiver. This work was completed by Fujiko Oguri as her masters thesis. Her work is summarized here as a paper submitted by Ohio University to these proceedings. Essentially, her work allows a complete implementation of the ability to navigate in a random fashion to any coordinates in the Loran-C coverage volume. The software provides cross-track error on a CDI, distance to go to the next waypoint, cross-track bearing, true course, ground speed and estimated time enroute. The Loran-C receiver with the RNAV software has been flight tested with excellent results.

Of particular significance is the fact that Ms. Oguri's thesis has been recognized by the Radio Technical Commission for Aeronautics (RTCA) through its W. E. Jackson Award for the outstanding technical paper submitted in the annual national competition. This is particularly noteworthy since the 1982 RTCA Jackson Award was presented to Joseph Fischer for his thesis supported by Joint University Program. His paper reported the design of the Loran receiver that was a prerequisite to Ms. Oguri's work with the RNAV. Importantly, both of these individuals have taken jobs in the avionics industry where their experiences with the Joint University Program is directly applicable.

New work that was begun in 1983 included a characterization of path differences for navigation equipment using great circle or rhumb-line course steering computations. Of major concern were the factors that controlled the cross-track path errors and the magnitude of the errors based on those factors. Rajan Kaul worked on a Fortran simulation that provided answers to these questions. This model will be implemented in the O.U. Loran-C receiver so that course steering can be provided based on rhumb-line as well as great circle. This issue of rhumb-line versus great circle becomes significant for situations where vehicles using navigation systems based on these different course computation methods begin to mix.

Additionally, Kaul is developing a microcomputer implementation of a model of the earth's magnetic variation to be included in the Ohio University Loran-C receiver software. This model implementation will allow automatic inclusion of the magnetic variation so that one less manual pilot entry is necessary.

In order to facilitate the necessary pilot data entry, a control display unit (CDU) is being developed for the Ohio University Loran-C receiver. This CDU will have the ability to not only present and absorb data but also to act as a window on other possible sensors and information systems on the aircraft. This is similar to the EFIS (Electronic Flight Instrumentation System) now available for some

aircraft. The CDU is designed to allow easy modification of the data entry and display so that new methods can be investigated with very little significant changes. This will certainly provide the necessary capability of this receiver.

The major purpose of this work is very close to being fully realized. This purpose, again, is to provide a research tool, a receiver, such that engineers interested in examining Loran-C performance, usefulness, and other properties will have a flexible, modifiable, and well-known piece of receiving hardware. Industry will, of course, have the opportunity to glean from the receiver system designs and products those items which will enhance their products and make Loran-C a more efficacious navigation system for the United States aviation community and possibly those communities with marine and land interests.

SUMMARY OF PAPER:

AREA NAVIGATION IMPLEMENTATION FOR A MICROCOMPUTER-BASED LORAN-C RECEIVER*

Fujiko Oguri
Ohio University
Athens, Ohio

The paper describes the development of an area navigation program and the implementation of this software on a microcomputer-based Loran-C receiver to provide high-quality, practical area navigation information for general aviation. This software provides range and bearing angle to a selected waypoint, cross-track error, course deviation indication (CDI), ground speed and estimated time of arrival at the waypoint. The range/bearing calculation, using an elliptical Earth model, provides very good accuracy; the error does not exceed more than 0.012 nm (range) or 0.09° (bearing) for a maximum range to 530 nm. The α-β filtering is applied in order to reduce the random noise on Loran-C raw data and in the ground speed calculation. Due to the α-β filtering, the ground speed calculation has good stability for constant or low-accelerative flight. The execution time of this software is approximately 0.2 second. Flight testing was done with a prototype Loran-C front-end receiver, with the Loran-C area navigation software demonstrating the ability to provide navigation for the pilot to any point in the Loran-C coverage area in true area navigation fashion without line-of-sight and range restriction typical of VOR area navigation.

*Published as TM 88 at Ohio University.

PAPER OUTLINE AND SCOPE

The following pages contain excerpts from Fujiko Oguri's paper. The scope and outline of the paper are shown below.

I. INTRODUCTION AND SUMMARY

II. PROBLEM DESCRIPTION

- A. Present-Day Navigation System
  1. VOR/DME system
  2. RNAV using VOR/DME system
  3. Other systems
- B. Low-altitude Navigation Using Loran-C

III. LORAN-C NAVIGATION

- A. Background
- B. Low Frequency System
- C. Loran-C Time Difference
- D. Computation of Time-Differences
- E. Converting Time-Difference
- F. Area Navigation

IV. COMPUTATION FOR AREA NAVIGATION

- A. Range and Bearing Angle
  1. Spherical model
  2. Simplified elliptical model
  3. Elliptical model
  4. Comparison among three models
- B. Other Navigational Information
  1. Cross-track error
  2. Ground speed and estimated time of arrival
- C. A Scheme for Microcomputer Use

V. THE MICROCOMPUTER SYSTEM

- A. A System Design
  1. Hardware
  2. Interfacing software
- B. Navigational Program
  1. Relationship among navigational programs
  2. RNAV program

VI. TESTS ON MICROCOMPUTER

- A. Testing with Simulations
- B. Flight Testing
  1. Filtering time differences
  2. Ground speed
  3. Range/bearing, CTE/CTEB and CDI indications

VII. CONCLUSIONS AND RECOMMENDATIONS

VIII. ACKNOWLEDGEMENTS

IX. REFERENCES

X. APPENDICES

- A. The Computation for An Area Navigation (RNAV) Equipment based on the use of VOR/DME
- B. Program Listing for Testing Range and Bearing Angle Computational Models
- C. Program Listing for Microprocessor Version of Area Navigation (RNAV) Program
- D. Program Listing for Testing Flight Test Data
- E. Program Listing for Testing Flight Test Data

PAPER EXCERPTS

The following excerpts (introduction, summary, conclusions, and recommendation sections) are shown on the following pages.

I. INTRODUCTION AND SUMMARY

This paper describes specific engineering work which has been done to make Loran-C a more useful and practical navigation system for general aviation. This work, in particular, deals with development of new software, and implementation of this software on a (MOS6502) microcomputer to provide high quality practical area navigation information directly to the pilot. Flight tests have been performed specifically to examine the efficacy of this new software. Final results were exceptionally good and clearly demonstrate the merits of this new Loran-C area navigation system.

LORAN-C (Long Range Navigation) is a hyperbolic, radio navigation system that has been in operation since 1958 [1]. It uses ground waves at low frequencies to provide positional information, not restricted to line-of-sight [2]. This system can be used in nearly all weather conditions to obtain position accuracies which are essentially independent of altitude. As of 1983, it is not yet a complete navigation system in the United States. In the midwest, which constitutes one third of the U.S. land area, coverage is deficient for some flight operations.

The VOR/DME (VHF Omni-directional Range/Distance Measuring Equipment) navigation system is well known as the contemporary, short-range navigation system which covers the whole United States with over 1000 stations, but this system is sensitive to siting and terrain, and has limits for low altitude coverage because VOR is a line-of-sight system. By relieving these shortcomings, Loran is considered to be a possible supplement for VOR/DME system [3].

The hyperbolic lines of position associated with Loran-C present a problem for the pilot. Historically, the hyperbolic lines of position do not convert readily to a meaningful display without comparatively high airborne equipment cost. However, the present availability of microprocessors makes low-cost airborne coordinate conversion equipment feasible. Contemporary technology provides for light-weight small-volume equipment with a low power drain for small aircraft. Thus, automatic Loran-C navigation can be made practical for general aviation users simply by making use of a microcomputer.

In this paper, work is described indicating rather elementary mechanizations that can provide the pilot very useful navigation at all altitudes. This development of software provides Area (Random) Navigation (RNAV) information from Time Differences (TDs) in raw form using an elliptical earth model and a spherical model. It is prepared for the microcomputer based Loran-C receiver which was developed at the Ohio University Avionics Engineering Center. In order to compute navigational information, a microcomputer(MOS6502) and a mathematical chip (Am9511A) were combined with the Ohio University Loran-C receiver. Final data in the report reveals that this software indeed provides accurate information with reasonable operation times.

VII. CONCLUSIONS AND RECOMMENDATIONS

Some specific conclusions can be reached as a result of the work performed in developing a microcomputer-based Loran-C receiver for general aviation application.

The objective of this area navigation software implementation is to provide high quality air navigation information by using Loran-C as a navigation system for general aviation. The following conclusions are made according to the test results in Chapter VI.

The conclusions are:

1. The high accuracy of the range/bearing calculation using the microcomputer-based Loran-C receiver was demonstrated; the error without a bias error does not exceed more than 0.012nm (range) or 0.09° (bearing) for ranges to 530nm.

2. Operational performance, as observed on a flight in a general aviation aircraft, is obtained using a α-β filter on time differences to reduce random noise. Filtering TDs with the new, stable clock, with an effective time constant is 4 seconds, effectively smooths the flight path and does not cause serious delay on the turns.

3. The ground speed calculation with 10 knots resolution has operational stability for a constant or low-acceleration flight. Since the ground speed calculation process passes through two filters, the ground speed cannot be easily updated with high acceleration. According to the effective time constants for the two filters (4 seconds for TDs and 12 seconds for the GS calculation), a step response becomes 86.3% of final value after 24 seconds. So the ground speed calculation can accept an acceleration which is less than $0.13 nm/s^2$.

4. The CTE/CTEB indication provides the relative position and proper direction respectively to any desired course inside the Loran-C coverage area. Even with an airplane very close to a To waypoint (less than 0.1nm) the CTE has sufficent sensitivity to calculate an accurate CDI indication, while the VOR navigation system at close range is too sensitive.

5. An execution time of the total navigation system routine does not exceed more than 1.5 seconds, which is short enough for adequate position update information for air navigation. In the northeast U.S. chain (GRI=99600μs), the execution time is about 1.39 seconds for RNAV position updates.

6. The Loran-C navigation system with the new stable clock recorded an average bias error of 0.5nm which meets the requirement stated in AC90-45A (enroute 2.5nm, terminal 1.5nm). Even for an approach, this system has the capability to meet the total error of 0.6nm stated in AC90-45A.

7. The Loran-C area navigation software makes it possible for the general aviation user to fly to any point inside the Loran-C coverage area in true area navigation fashion unlike VOR navigation system with its line-of-sight and range restrictions.

Some problems were identified during the testing, and these should be addressed and solved prior to implementation by general aviation.

1. The bias error to the north is due to signal-strength differences of Loran-C stations and Avionics Engineering Center's receiver implementation. The bias error can be significantly reduced with a new RF front end [42] and applying propagation corrections. The recent tests with the new RF front end indicated a bias error of 0.2nm. These data were collected in the same area as the previous flight tests. The bias error of 0.2nm could be further reduced with the application of a propagation correction.

2. An improved ground speed response for accelerated flight. The ground speed response for accelerated flight can be improved by implementing a three dimensional filter [43]; however, improvement of measuring time differences to reduce random noise should be made to provide better data for ground speed calculations.

Contemporary microprocessor technology has greatly improved the capability for quality high navigation, and allows for achieving low-cost and light weight receivers for general aviation applications. This RNAV software promises to provide the pilot with significant operational advantages through the use of a microcomputer-based Loran-C receiver.

MODIFIED TIMING MODULE FOR LORAN-C RECEIVER*

Robert W. Lilley
Ohio University
Athens, Ohio

I. ABSTRACT

Hardware documentation is provided for the modified Loran-C timing module, which uses interrupt-driven software control in determining loop sample times. Computer loading is reduced by eliminating polled operation of the timing loop.

II. SUMMARY

The original design for the Ohio University Loran-C receiver featured a software/hardware locked-loop signal processor, based upon the Mostek 50395 timing integrated circuit (IC) [1,2]. This IC provides a six-digit binary-coded decimal (BCD) counter and a BCD register compared to generate an output pulse when the register and counter contents are equal. Operated at 1 MHz, this timing circuit permits microcomputer-selected sample times to be precisely set within a one-second counter interval, with a resolution of one microsecond.

In order to accomplish the data load for the IC register, the computer must detect that the IC digit scan oscillator has selected the appropriate 4-bit BCD digit, and then strobe the new digit data into the register. The IC design requires a scan oscillator frequency of no higher than 20 kHz, which places a lower limit on the time required to load all six digits. In practice, the complete register load requires approximately 500 microseconds (μs).

The original receiver design makes all six IC digit strobe signals available to the microcomputer, which then strobes the new digit data into the register after detecting the presence of the appropriate strobe signal. This operation must take place in order to preset the next loop sample time, triggered by the EQUAL pulse from the Mostek IC. Therefore, the register load must be performed between each Loran-C pulse. The technique of polling the digit strobe lines to detect the next digit to be loaded requires full attention from the microcomputer, delaying background processing.

The modified circuit described in this technical memorandum combines all six-digit strobes into one master strobe signal, which appears as an interrupt to the microcomputer. Therefore, once a digit is loaded into the IC register, the computer is free to process background code while awaiting the next digit strobe interrupt. See figure 1 for a block diagram.

---

*Published as TM 87 at Ohio University.

This modification is required, to permit the single processor (a MOS Technology 6502) to perform all required computations for the entire Loran-C process. Expansion of the receiver from a three-station tracker to full five-station operation would cause over 20 percent of processor power to be lost to the strobe polling operation, causing a reduction in navigation data output rates, and a reduction in the number of pilot-oriented features which could be added using the single processor.

Full hardware documentation is provided in this document for the circuit card implementing the Loran-C timing loop, and the receiver event-mark and re-track functions. This documentation is to be combined with overall receiver drawings to form the as-built record for this device. Computer software to support this module is integrated with the remainder of the receiver software, in the LORPROM program.

III. CIRCUIT DESCRIPTION

Figure 2 shows the complete logic diagram for the Loran-C timing module. To the far left are signal descriptors for the system computer, an MAI SuperJolt based upon the MOS Technology 6502 with 6520 peripheral interface adapter (PIA). All connections, except for CLOCK and IRQ, are made through the 6520 PIA. Figure 3 gives a summary of PIA pin assignments, useful in software design and coding. The Mostek 50395 chip description is given as figure 4, and pinouts are shown in figure 5.

Referring to figure 2, note that seven lines provide data and control signals to the Mostek IC (U3). All these signals are output by the computer as TTL-compatible signals, and must be changed to the 12-volt MOS specification required by U3. This conversion is performed in open-collector drivers U1 and U2, pulled up to 12v through 680-ohm resistors. These lines carry the four data bits for register digits Ra, Rb, Rc and Rd. The LR (Load Register) strobe and $\overline{\text{SET}}$ (Set digit counter to most-significant digit) signals.

The timing chip U3 is wired for free-running counter, counting up, and is driven by the CLOCK, which is a buffered version of the main microcomputer clock (a temperature-compensated crystal oscillator). The scan oscillator which generates the digit strobes to indicate the load window for each register digit is set to 20 kHz using the capacitor at pin 21. Digit strobes, one for each register BCD digit, are output by U3 at pins 24 through 29 and are immediately NORed by U6. Note that this 8-input NOR is a CMOS chip running at 12v to eliminate the need for the six voltage dividers used in the previous design to return the MOS levels from U3 to TTL levels. The combined digit strobe is then returned to TTL levels, inverted by U7 and applied as a clock to the U8 D flip-flop latch.

The Q output of the U8 latch is high after receipt of a digit strobe, which causes the output of the U7 interrupt combiner gate to go low, causing an interrupt (IRQ) condition at edge connector pin 19. Once the computer program has serviced this interrupt, the digit strobe interrupt latch U8 is cleared by a low signal at $\overline{\text{CLRD}}$, or pin 12. The computer software simply counts interrupts from the digit strobe latch, recognizing that the digit strobes appear in fixed order from digit one through six.

Appropriate signals are then placed on the Ra - Rd lines and the U3 control lines to achieve the full register load.

Once the register is fully loaded, the digit strobe interrupts are disabled by placing a low level on $\overline{CLRD}$, forcing the U8 latch into reset condition. The U5 Loran-C interrupt and data latches are then enabled by bringing $\overline{CLRP}$ high. When the free running counter in U3 reaches the register value just loaded, U3 issues an EQUAL pulse for one clock period (one μs) which clocks the U5 latches. The output of the IRQ combiner gate in U7 goes low since the Q output of the U5 interrupt latch always goes high upon clocking. An interrupt is signaled at $\overline{IRQ}$ to the computer. LDAT, latched by the U5 Loran-C latch, assumes the instantaneous value of the Loran-C digital waveform received at $\overline{LRIN}$ from the receiver front-end module. Note that $\overline{LRIN}$ is processed by U4 to set a pulse width of approximately 70 μs. before it is sampled. This pulse width is necessary to provide a guard time after the leading pulse edge to permit successful pulse tracking, and to minimize initial search time. Since the various front-end processors designed to date have presented various pulse widths, this U4 mono-stable multivibrator has been provided to equalize the waveform before sampling.

The remainder of the circuit, U12, deals with receiver features included for evaluation. The event latch is driven by a front-panel pushbutton to place on the receiver output tape a unique mark so output data may be correlated with flight events. The retrack latch, also operated by pushbutton, signals the computer that the operator wishes to restart the Loran-C search process. To minimize contact bounce, these latches are configured to operate on the pushbutton release cycle.

Once the computer program has serviced the Loran-C sample interrupt thus generated, the U5 latches are disabled by a low at $\overline{CLRP}$ and the digit strobe interrupt is enabled by a high on $\overline{CLRD}$. Another register load sequence begins.

In this manner, successive samples may be taken of the Loran-C input waveform at times which are precisely controlled by the microcomputer. The programmer may now select algorithms for detecting received Loran-C chains and stations by varying the sample time and observing the result at LDAT.

The module pictorial appears in figure 6, giving placement of ICs and other major components.

IV. REFERENCES

[1] Lilley, R. W. and D. L. McCall, "A Loran-C Prototype Navigation Receiver for General Aviation," paper (No. 81-2329), presented at the AIAA/IEE Fourth Digital Avionics Systems Conference, November 1981.

[2] Lilley, R. W. and D. L. McCall, "A Loran-C Prototype Navigation Receiver for General Aviation," (NASA) Technical Memorandum 80, Avionics Engineering Center, Department of Electrical and Computer Engineering, Ohio University, August 1981.

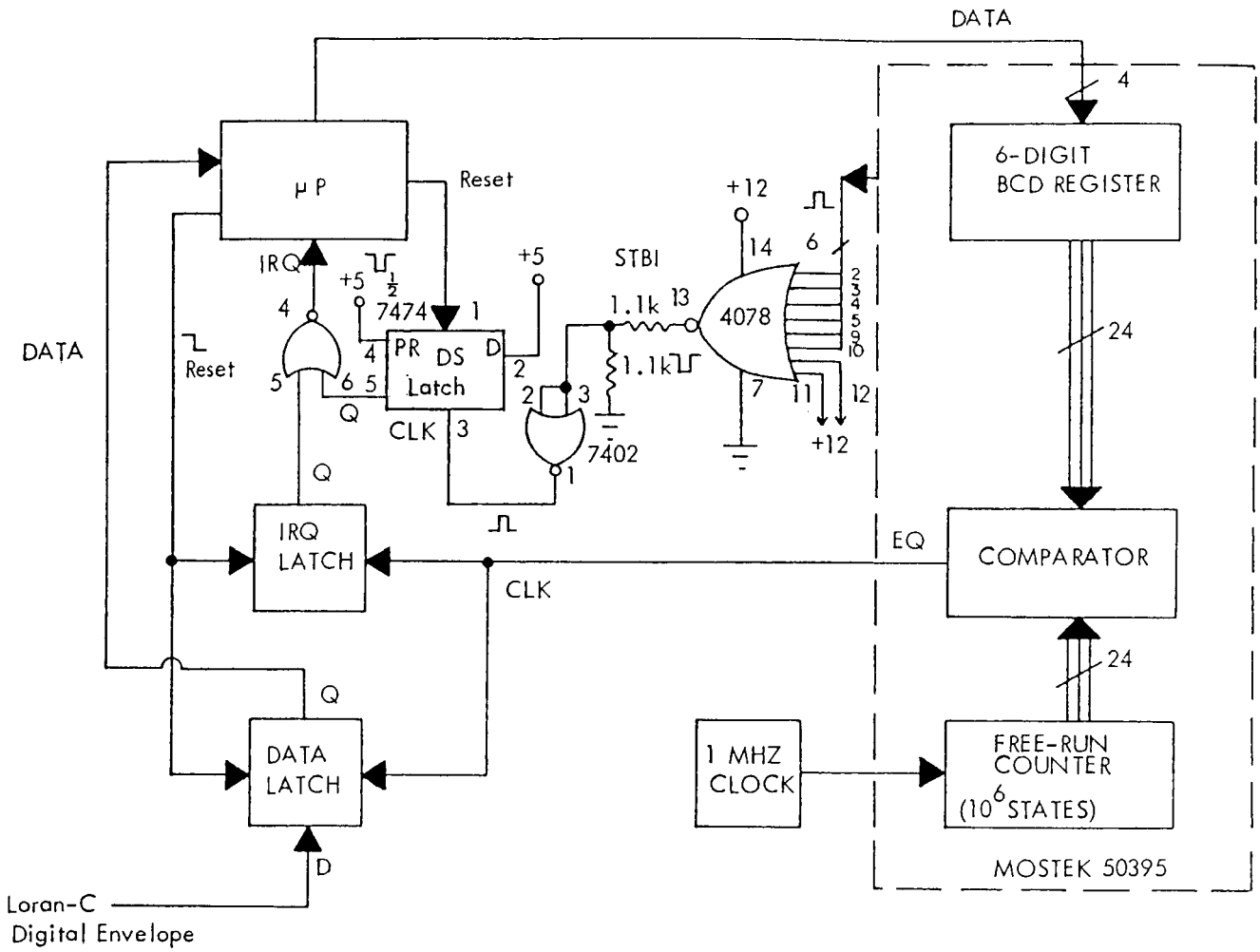

Figure 1. Block diagram, Loran-C timing module.

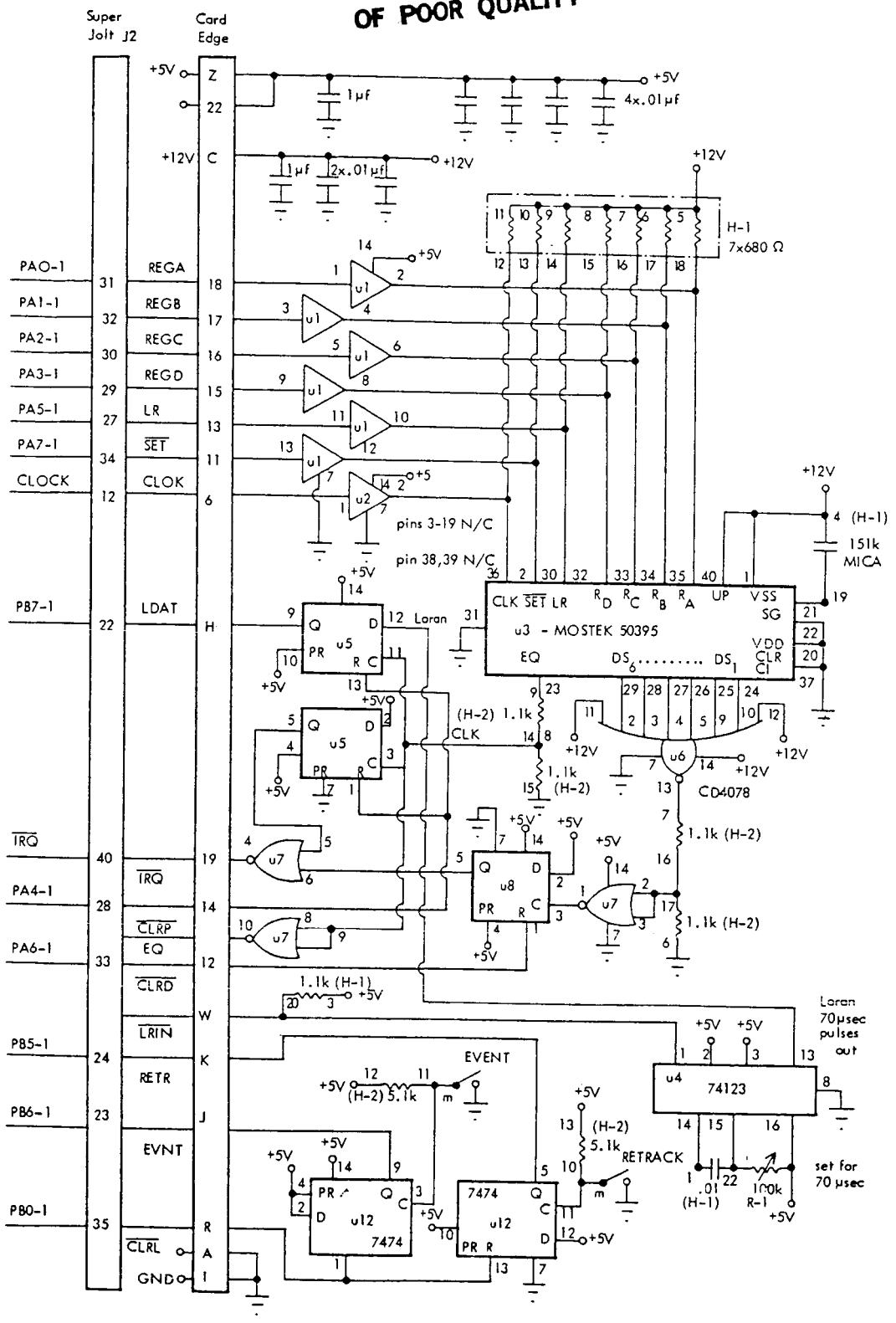

Figure 2. Loran-C timing board for updated RF board only.

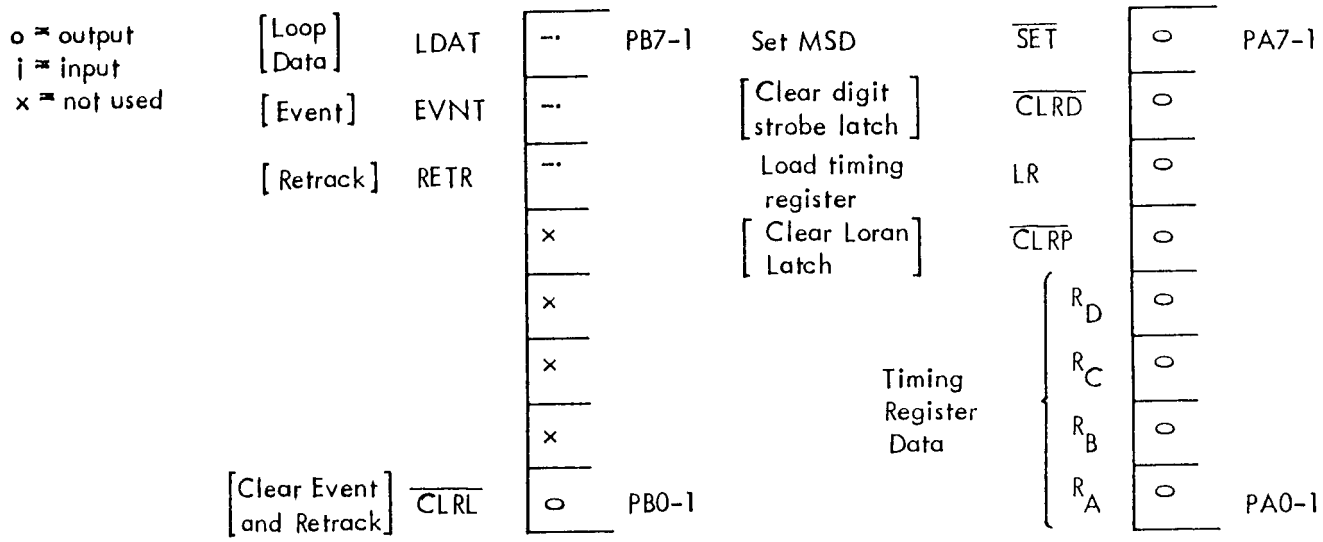

Figure 3. SuperJolt to timing board summary of PIA assignments.

FUNCTIONAL DIAGRAM

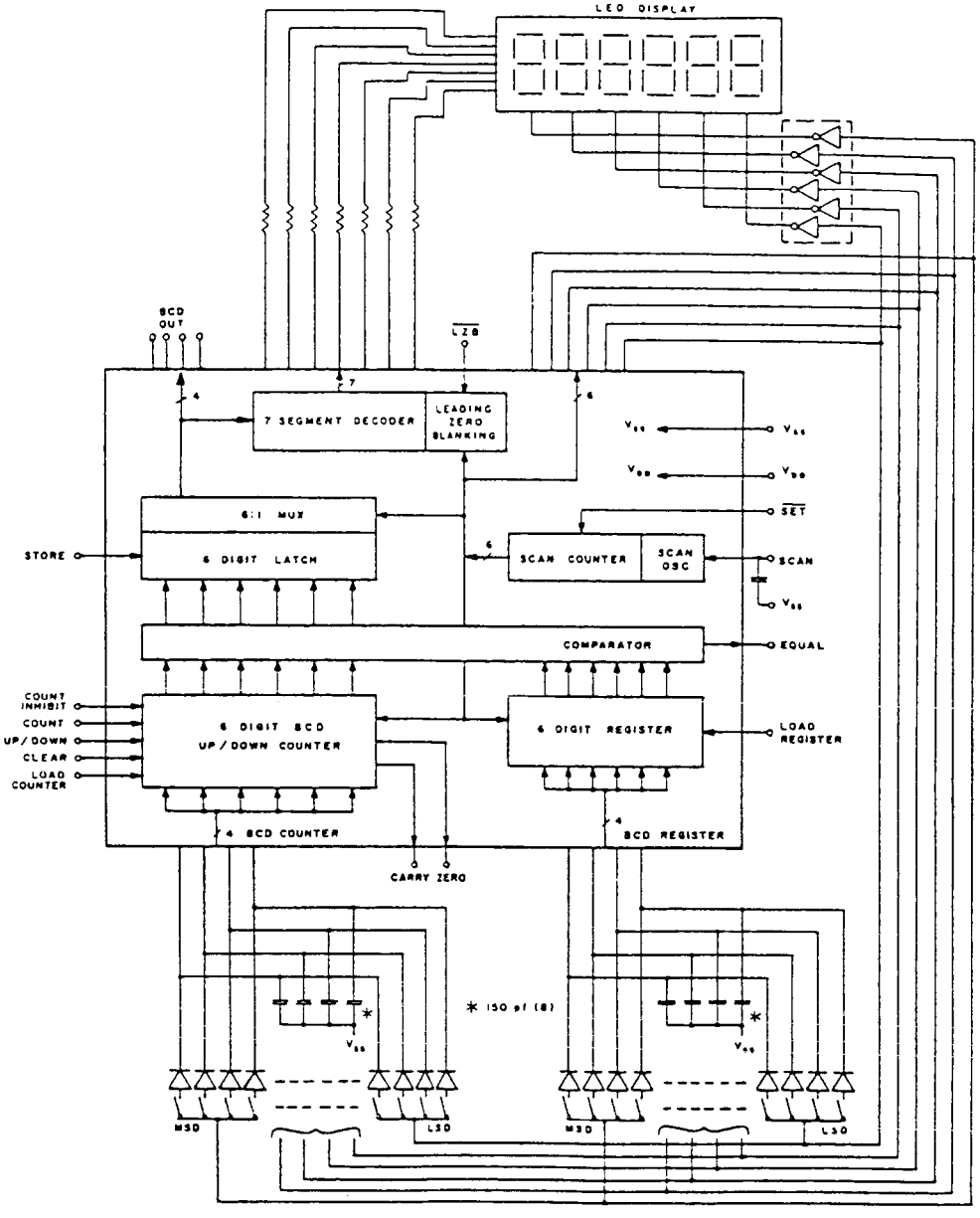

Figure 4. MOSTEK 50395 integrated circuit.

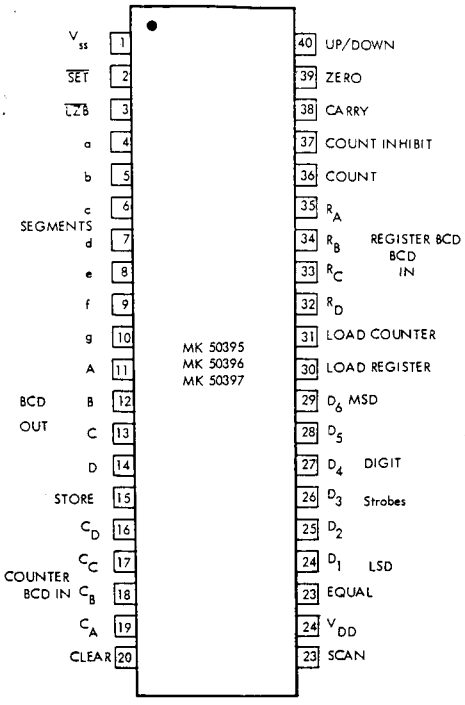

Figure 5. MOSTEK 50395 pinouts.

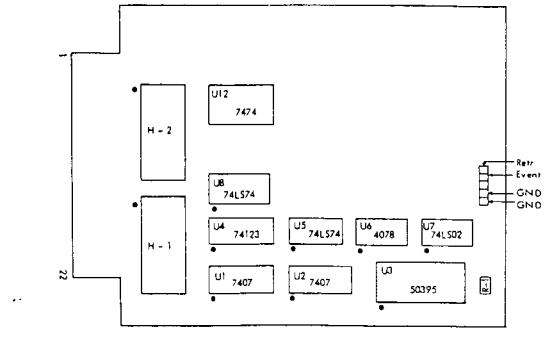

Pin	Signal	Description
R	$\overline{CLRL}$	Low clears retrack & event latches.
J	EVNT	High indicates user event mark, cleared by $\overline{CLRL}$.
K	RETR	High indicates user retrack, cleared by $\overline{CLRL}$.
W	$\overline{LRIN}$	Input Loran-C pulses from front-end. TTL, open-collector, pulled up to 5V on this board
18	REGA	4-bit BCD digit load for U3 register.
17	REGB	
16	REGC	
15	REGD	
13	LR	Load 50395 (U3) Register strobe.
11	$\overline{SET}$	Set U3 to MSD for data load.
6	CLOK	1 MHz clock, from microcomputer.
12	$\overline{CLRD}$	Low clears digit strobe IRQ latch.
14	$\overline{CLRP}$	Low clears Loran data latch.
H	LDAT	Loran data - loop sample output.
19	$\overline{IRQC}$	Combined IRQ from loop and digit strobes.
V	EQ	Equal pulse, for monitoring.

Figure 6. Pictorial and signal glossary.

PATH DISCREPANCIES BETWEEN GREAT CIRCLE AND RHUMB LINE*

Rajan Kaul
Ohio University
Athens, Ohio

A simulation of a mathematical model to compute path discrepancies between great circle and rhumb line flight paths is presented. The model illustrates that the path errors depend on the latitude, the bearing, and the trip length of the flight.

I. INTRODUCTION

A mathematical model for a comparative analysis of great circle versus rhumb line navigation in the continental United States has been developed at the Avionics Engineering Center, Ohio University. A FORTRAN simulation of the model has been implemented on the IBM 370 computer. The simulation predicts pertinent navigation information for the two flight paths. The basis for the project, which is a part of an M.S. thesis, is to provide a data base for computing discrepancies between the two flight paths. This document briefly describes the model and discusses the implications of the results obtained.

II. BACKGROUND INFORMATION

The standard en-route navigation system used in the United States is the VOR/DME. VHF Omnidirectional Range (VOR) is the basis for defining the airways and is therefore an integral part of air traffic control procedures. Two VOR stations are used to define a radial intersection, which is the basis of the established Victor airways. These Victor airways follow a flight path which maintains a path of constant heading (i.e. the course crosses the meridians at the same angle). Thus, a rhumb line course appears as a straight line on a Mercator projection.

Area/Random Navigation (RNAV) as defined in FAA Advisory Circular 90-45A (1) is

> '...a method of navigation that permits aircraft operations on any desired course within the coverage of station referenced navigation signals or within the limits of self-contained system capabilities.'

The principal advantage of RNAV is that it allows the navigator to fly a great circle course between two points. The great circle course is the

*Published as TM 89 at Ohio University.

shortest path between two points on the earth, and is formed by the intersection of the plane defined by the center of the earth and the points of origin and destination, projected on the surface of the earth. The flight path is projected as a curved line on a Mercator projection and hence changes heading constantly.

Loran-C, OMEGA, GPS, Doppler, and INS are considered RNAV systems. However, VOR in its basic form is not an RNAV system. A major concern is that the discrepancies between the two flight paths may cause navigation conflicts. This report attempts to quantize the discrepancies which depend on various factors.

III. PATH DISCREPANCIES

The magnitude of path discrepancies between the great circle and rhumb line courses between two points increases as

1) the latitude increases,
2) the difference in their latitudes decreases and
3) the difference in their longitudes increases.

When plotted on a Mercator projection map, the two flight paths start to diverge from the origin of the flight. The discrepancy is a maximum at the mid-point of the flight, and then the flight paths start to converge and meet at the destination point. The great circle path is always curved away from the equator and therefore intersects the meridians at higher latitudes than the rhumb line path. Also, the meridians converge as they depart from the equator and are closer together at higher latitudes. Thus, the deviation between the two paths increase at higher latitudes because the rhumb line path must curve rapidly to be able to fly a course of constant meridian crossing angle.

The bearing of the flight path, which is a simple function of the latitude and longitude, also has a considerable effect on the discrepancies between the two flight paths. By definition, all lines of longitude are also great circles. On a true north-south flight path the great circle and rhumb line courses are exactly the same. However, as the bearing becomes more easterly or westerly, errors between great circle and rhumb line paths start to increase. The maximum path errors due to bearing alone are on a true east-west course. It is important to note that on an east-west course at the equator the great circle and rhumb line flight paths are the same because the equator is also a great circle path.

Finally, another factor that has an effect on path discrepancy is the trip length, which is also a function of the latitude and longitude of the two points. As mentioned earlier, the great circle and rhumb line courses start to diverge from the point of origin of the flight and reach the point of maximum divergence half way into the flight. Therefore, as the trip length increases the paths simply diverge further till they reach the halfway point.

IV. THE MODEL

The mathematical model which was developed using the haversines formula was obtained from Bowditch (2). The equations developed for the model were designed for computer applications. The model is based upon a spherical approximation of the earth and adjusted using geodesic error equations for the North American datum based on the Clarke ellipsoid. The equations describing the model are given below.

ϕ_1 = Latitude of origin in degrees

λ_1 = Longitude of origin in degrees

ϕ_2 = Latitude of destination in degrees

λ_2 = Longitude of destination in degrees

$\overline{\phi} = \frac{(\phi_1 + \phi_2)}{2}$ --- mid-latitude point

$Dlo = \lambda_2 - \lambda_1$ --- difference in longitude

Dlox = Interval of longitude measured from point of departure in degrees

A. RHUMB LINE EQUATIONS

Rhumb line bearing (relative from origin to destination)

$$\alpha = Tan^{-1} \left(\frac{\phi_2 - \phi_1}{Dlo \cdot Cos\phi} \right)$$

Latitude of points on a rhumb line path

$$\phi_{(RL)} = \phi_1 + Dlox \cdot Cos\overline{\phi} \cdot Tan\alpha$$

Rhumb line distance

$$RLDIST = 60\sqrt{[(\phi_2 - \phi_1)^2 + (Dlo \cdot Cos\bar{\phi})^2]}$$

B. GREAT CIRCLE EQUATIONS

Initial course of the great circle path

$$C = Tan^{-1}\left(\frac{Sin(Dlo)}{Cos\phi_1 \cdot Tan\phi_2 - Sin\phi_1 \cdot Cos(Dlo)}\right)$$

Vertex

The vertex is the point of highest latitude on a great circle path

$$Lv = Cos^{-1}\,[Cos(\phi_1) \cdot Sin(C)]$$

Difference in longitude between vertex and point of origin

$$Dlov = Sin^{-1}\left[\frac{Cos(C)}{Sin(Lv)}\right]$$

Latitudes of points on great circle path

$$\phi_{(GC)} = Tan^{-1}\,[Tan(Lv) \cdot Cos(Dlox - Dlov)]$$

Great circle distance

$$GCDIST = 60 \cdot Cos^{-1}\,[Sin(\phi_1) \cdot Sin(\phi_2) + Cos(\phi_1) \cdot Cos(\phi_2) \cdot Cos(Dlo)]$$

C. GEODESIC ERROR EQUATIONS

The geodesic error equations between the model and Clarke ellipsoid

$$\text{ERROR(east)} = [9.12951 \cdot \text{Cos}(\bar{\phi}) - 2.92495 \cdot \text{Cos}(3\bar{\phi})] \cdot (\lambda_2 - \lambda_1) \cdot \frac{\pi}{180}$$

$$\text{ERROR(north)} = 0.37414 \cdot (\phi_2 - \phi_1) \cdot (\frac{\pi}{180}) - 8.88543 \cdot [\text{Sin}(2\phi_2) - \text{Sin}(2\phi_1)]$$

Similar equations were also used by Hogle, Markin and Toth in their report 'Evaluation of Various Navigation Concepts' (3).

V. RESULTS AND CONCLUSIONS

The equations detailed in the previous section were modeled in FORTRAN on the Ohio University IBM 370 computer. Figures 1 and 2 are simulations of great circle and rhumb line paths on a mercator projection. The results indicate that the discrepancy between the two flight paths can be significant. Figure 1 is an east-west flight path from Baltimore-Washington International to Los Angeles International airport. At the point of maximum deviation the path discrepancy is 126 nautical miles for a trip length of 2017 nmi. On the other hand, a north-south flight path from St. Paul to Houston the discrepancy at the point of maximum deviation is only 5.25 nmi for a trip length of 903 nmi. (Figure 2.)

Since shorter trip lengths are of major importance to the pilot an effort was made to quantify the path errors for flight paths of up to 500 nmi. Figures 3 through 6 illustrate how the factors mentioned earlier effect the path discrepancies. The flights were simulated at a constant bearing with the mid-point of the flight at the specified latitude. Comparisons of the plots indicate the compound effect bearing and latitude of the mid-point of a flight have on the path errors. A flight at a mid-point latitude of 35 degrees north and a relative bearing of 76 degrees has maximum path errors of 1.1 nmi for trip lengths of up to 300 nmi (Fig. 3). However, a flight at the same mid-point latitude, but a relative bearing of 39 degrees has maximum path errors of more than 6 nmi for trip lengths up to 450 nmi (Fig. 5).

It is of vital importance to note here that the errors mentioned in this report are solely due to the discrepancies in the great circle and rhumb line paths. The errors do not account for reciever computational errors or pilot errors. Another source of error may be discrepancies among the earth models in various RNAV recievers. Offsets due to using different navigation systems in the same airspace also may cause considerable disparity (4). It is recommended that any decision made regarding this subject must take into account all discrepancies mentioned above, and not just the goemetrical errors.

VI. ACKNOWLEDGMENTS

This work presented in this technical memorandum has been supported by the National Aeronautics and Space Administration-Langley Research Center and the Federal Aviation Association under grant number NGR 36-009-017. It was performed at Ohio University's Avionics Engineering Center.

The author would like to acknowledge the help of Dr. Robert Lilley Associate Director, and Mr. James Nickum project engineer at Avionics Engineering Center, whose suggestions proved invaluable in all stages of this research.

VII. REFERENCES

[1] "Advisory Circular," Department of Transportation/Federal Aviation Adminstration, AC 90-45A, Feburary, 1975.

[2] Bowditch, N., "American Practical Navigator," Defense Mapping Agency Hydrographic Center, 1977.

[3] Hogle, L., Markin, K., and Toth, S., "Evaluation of Various Navigation System Concepts," prepared for Department of Transportation, Federal Aviation Adminstration, Report No. FAA-EM-82-15.

[4] Ibid.

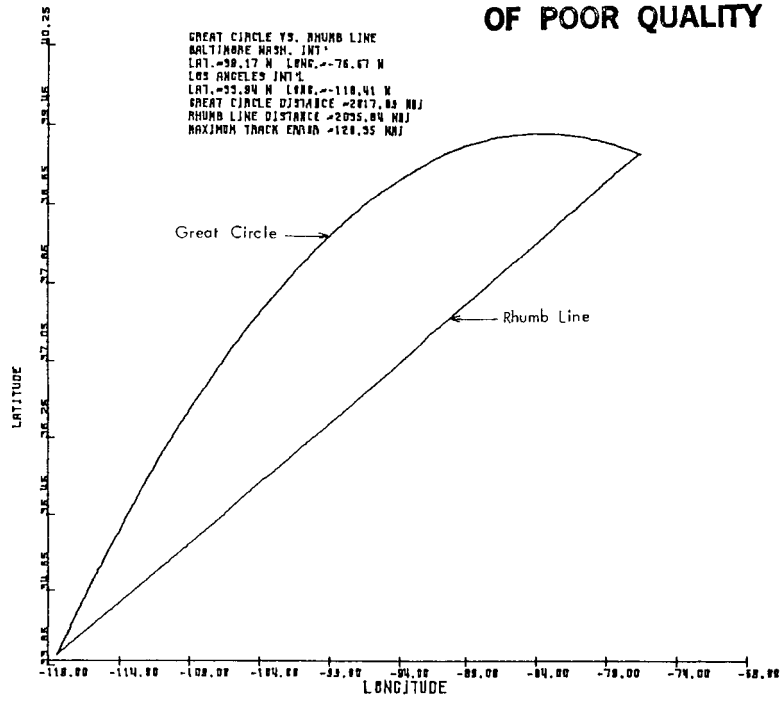

Figure 1. Great circle versus rhumb line. Baltimore - Washington to Los Angeles.

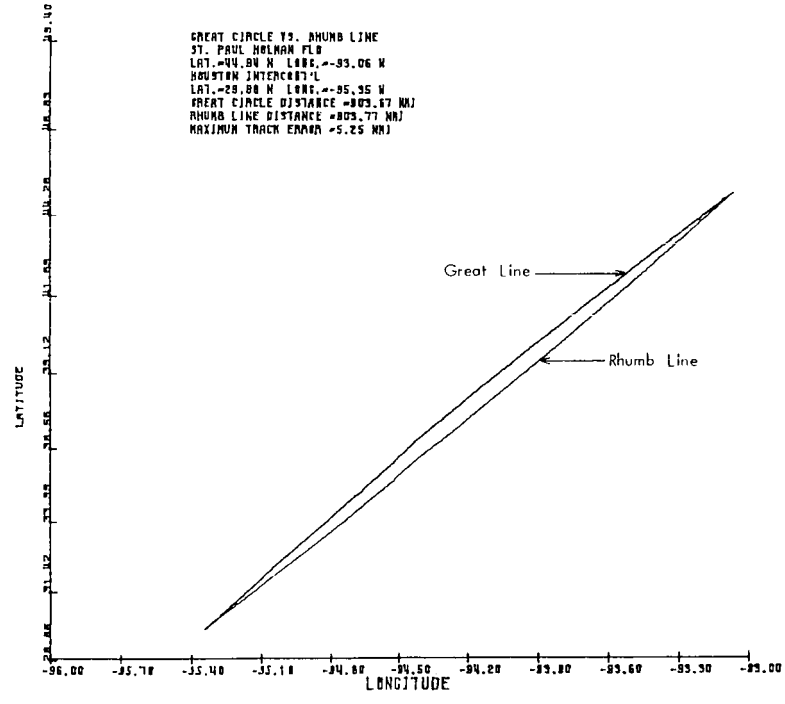

Figure 2. Great circle versus rhumb line. St. Paul to Houston.

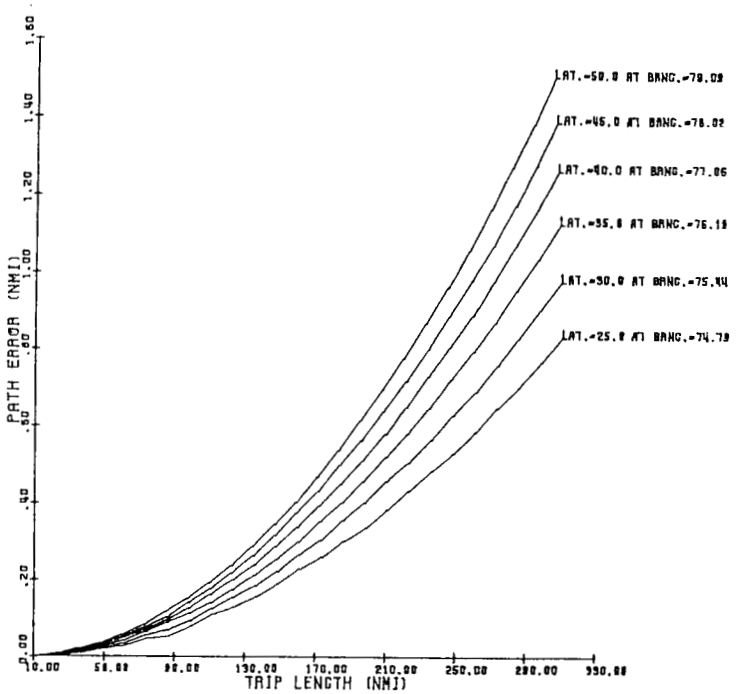

Figure 3. Path errors versus trip length at average bearing 76°.

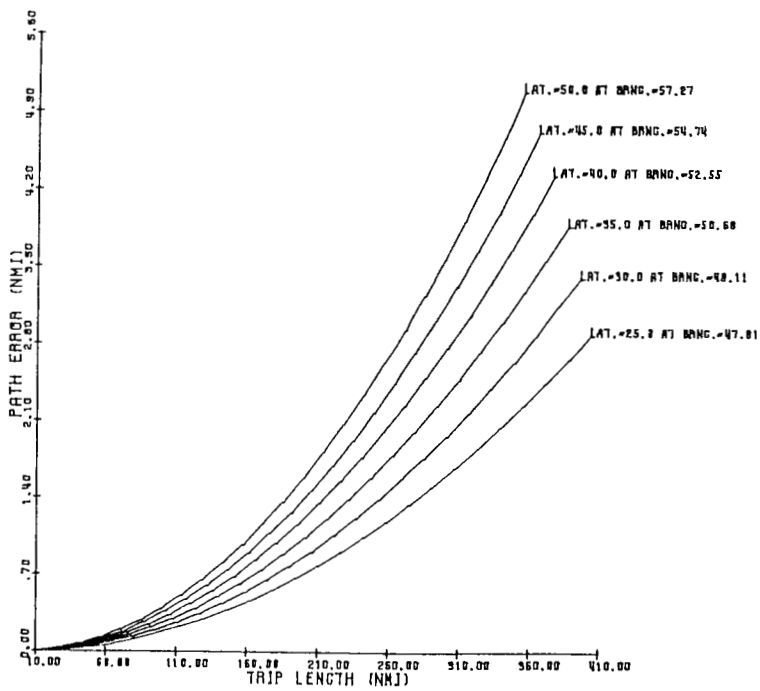

Figure 4. Path errors versus trip length at average bearing 52°.

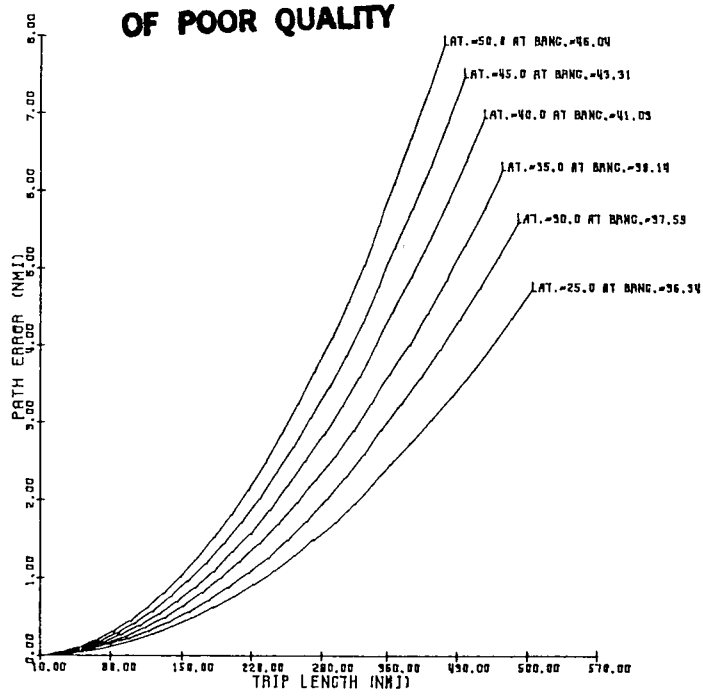

Figure 5. Path errors versus trip length at average bearing 40^{o}.

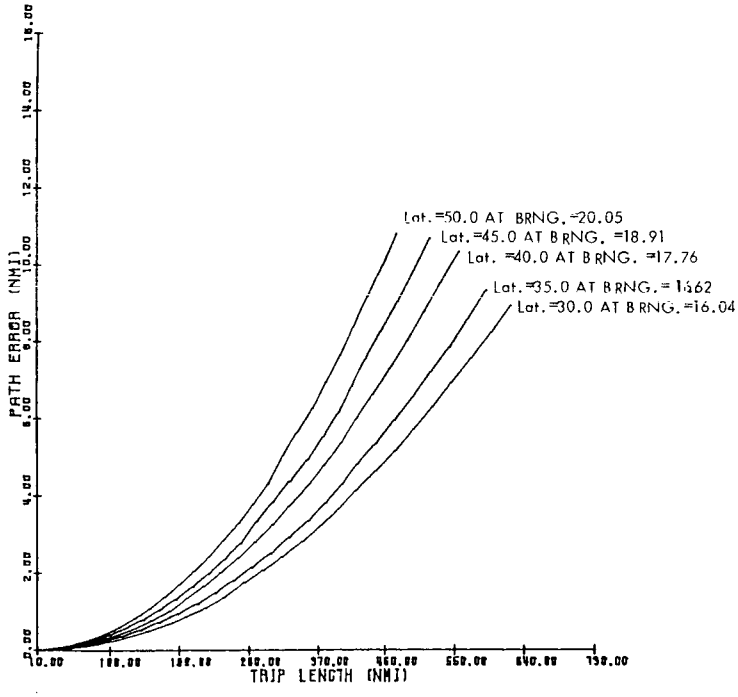

Figure 6. Path errors versus trip length at average bearing 18^{o}.

INVESTIGATION OF AIR TRANSPORTATION TECHNOLOGY AT PRINCETON UNIVERSITY, 1983

Robert F. Stengel
Department of Mechanical and Aerospace Engineering
Princeton University
Princeton, New Jersey

SUMMARY OF RESEARCH

The Air Transportation Technology Program at Princeton University, a program emphasizing graduate and undergraduate student research, proceeded along four avenues during 1983:

- Voice Recognition Technology for Flight Control
- Guidance and Control Strategies for Penetration of Microbursts and Wind Shear
- Application of Artificial Intelligence in Flight Control Systems
- Computer-Aided Aircraft Design

Areas of investigation relate to guidance and control of commercial transports as well as general aviation aircraft. Interaction between the flight crew and automatic systems is a subject of principal concern.

Computerized voice recognition of pilot inputs could play a major role in future air transportation. This capability has particular significance for single-pilot instrument-flight operations, where one pilot is required to perform all the tasks normally assigned to two or three persons in a larger aircraft. The tasks that can be carried out using voice command are varied; as a generality, they can be characterized as the jobs that a captain might ask the co-pilot to do, e.g., tuning radios, maintaining contact with air traffic control, holding altitude, and performing system status checks. Graduate student Chien Huang conducted flight tests in which the DME radio of Princeton's Avionics Research Aircraft was tuned by voice {1}. Tuning was accomplished by sending digital signals from a microprocessor, which received inputs from the pilot via the microphone and voice recognition board. Initial developments were extended to include the statistical evaluation of the system when used with different vocabularies, operators, and background noise conditions.

Recently, it has become apparent that severe downdrafts and resulting high velocity outflows present a significant hazard to aircraft on takeoff and final approach. This condition is called a microburst, and while it often is associated with thunderstorm

activity, it also can occur in the vicinity of dissipating convective clouds that produce no rainfall at ground level. Microburst encounter is a rare but extremely dangerous phenomenon that accounts for one or two air carrier accidents and numerous general aviation accidents each year (on average). Conditions are such that an aircraft's performance envelope may be inadequate for safe penetration unless optimal control strategies are known and applied. While a number of simulation studies have been directed at the problem, there are varied opinions in the flying community regarding the best piloting procedures, and optimal control strategies remain to be defined.

Graduate student Mark Psiaki has undertaken a study of guidance and control strategies for penetration of microbursts when encounter is unavoidable. It appears that the scale of meteorological activity that presents the greatest hazard for transport-type aircraft is quite different from that for general aviation aircraft. Nevertheless, preliminary investigation has revealed commonalities in control laws that reduce altitude response to microbursts {2}. Professor Stengel also contributed to the National Research Council report on the subject {3}.

Undetected system failures and/or inadequately defined recovery procedures have contributed to numerous air carrier incidents and accidents. The infamous DC-10 accident at Chicago's O'Hare Airport, in which loss of an engine pod, subsequent loss of subsystems, and asymmetric wing stall led to disaster, provides a prototype for the kind of tragedy that could be averted by intelligent flight control systems. (An intelligent control system is one that uses artificial intelligence concepts, e.g., an expert systems program, to improve performance and fault tolerance.) Although many methods of modern control theory are applicable, the scope of the problem is such that none of the existing theories provides a complete and practical solution to the problem. At the same time, heuristic logic may be applicable, but it has yet to be stated in satisfactory format.

As a first step in our investigation, graduate student Francois Dallery has completed an M.S.E. thesis on reconfigurable flight control systems {4}. In this work computer simulations verify the ability of relatively simple logic to detect and identify failures in flight control systems and in the airframe itself. Graduate student David Handelman is continuing this work with the design of a knowledge-based reconfigurable flight control system that will be implemented using parallel microprocessors.

Work was continued on the Princeton Aircraft Design System (PADS), a modular interactive graphics computer program for the design of aircraft. The objective is to facilitate the design of aircraft configurations ranging from general aviation and glider aircraft to supersonic transports and other high-performance aircraft. Two students produced reports on various aspects of the PADS computer program, which is implemented in the APL computer

language using Princeton University's IBM 3081-based Interactive Computer Graphics Laboratory facilities {5,6}. Seniors John Schneider and Brian Holasek completed program modules for three-dimensional display of aircraft configurations and for the design of wing and tail components.

Additional documentation of prior work occurred during the year. A paper on the use of fiber optics in flight control systems appeared in the IEEE Transactions on Aerospace and Electronic Systems {7}, while a summary of work on flying qualities criteria for single-pilot instrument flight was presented at the SAE Business Aircraft Meeting and Exposition {8}.

The NASA grant supporting student research in air transportation technology has inestimable value in helping educate a new generation of engineers for the aerospace industry, and it is producing research results that are relevant to the continued excellence of aeronautical development in this country.

REFERENCES AND ANNOTATED BIBLIOGRAPHY

1. Stengel, R.F., and Huang, C.Y., "Flight Tests of Voice Recognition Technology", presented at a Meeting of the Voice Technology for Systems Application Subgroup of the Department of Defense Human Factors Engineering Technical Advisory Group, Fort Monmouth, Oct 1983.

   A commercially available voice-recognition module was used to tune a DME navigation system in flight tests of Princeton University's Avionics Research Aircraft (ARA). The ARA is a fly-by-wire aircraft that is equipped with a digital flight control and data acquisition system; microprocessor-based systems installed in the aircraft facilitated integration of the voice-recognition unit, and initial tests proceeded at a rapid pace. Experimental error rates were no greater than those associated with manual inputs, and subsequent laboratory tests have indicated areas for further improvement.

2. Psiaki, M.L., and Stengel, R.F., "Analysis of Aircraft Control Strategies for Microburst Encounter", AIAA Paper No. 84-238, Aerospace Sciences Meeting, Reno, Jan 1984.

   Penetration of a microburst during takeoff or approach is an extreme hazard to aviation, but analysis has indicated that risks could be reduced by improved control strategies. Attenuation of flight path response to microburst inputs by elevator and throttle control was studied for a jet transport and a general aviation aircraft using longitudinal equations of motion, root locus analysis, Bode plots of altitude response to wind inputs, and nonlinear numerical simulation. Energy management relative to the air mass, a pitch-up response to decreasing airspeed, increased phugoid-mode damping, and decreased phugoid natural frequency were shown to improve microburst penetration characteristics. Aircraft stall and throttle saturation were found to be limiting factors in an aircraft's ability to maintain flight path during a microburst encounter.

3. Townsend, J., ed., Low-Altitude Wind Shear and Its Hazard to Aviation, National Research Council Committee Report, National Academy Press, Washington, 1983.

   The committee reviewed the state of knowledge about low-altitude wind shear, studied the hazards of low-altitude wind variability, and recommended actions to reduce the hazards of wind-shear encounters. A principal finding was that low-altitude wind variability presents an infrequent but highly significant hazard to aircraft during takeoff and landing; when

significant wind shears are known to be present, pilots should avoid flight into the area. In the near term, risks can be reduced by improving and automating the Low-Level Wind Shear Alert System (LLWSAS) and by installing the system at more airports. Education and training of pilots about wind-shear hazards are inadequate and should be improved. Better information is required concerning the response to wind shear of aircraft of various categories and sizes, taking account of the effects of piloting techniques and guidance and control systems. Utilization of ground-based Doppler weather radar would enhance detection of wind shear in the terminal area. Research should be conducted on the meteorological phenomenon, on the effects of heavy rain on aircraft aerodynamics, and on airborne wind-shear detection systems.

4. Dallery, F., "Failure Detection and Identification for a Reconfigurable Flight Control System", M.S.E. Thesis, Princeton University Report No. MAE-1639T, Nov 1983.

This thesis presents a fault-tolerant control system architecture that uses analytical and parallel redundancy to achieve failure detection, identification, and system reconfiguration. The proposed system has been developed and tested through extensive numerical simulations. The procedure is applied to a mathematical model of a transonic executive jet aircraft. The control system is found to provide excellent stability for standard aircraft sensors of comparable noise levels, and performance is found to be sensitive to control sampling interval.

5. Schneider, J., "PADS Multi-View Display Package", Princeton University Senior Independent Work Project Report, Jan 1983.

This multi-view display package uses a node-link data base to list, store, and retrieve designs. It displays three-view and oblique-view representations of an object described as an assemblage of polygons. Graphic examples for a simple aircraft configuration are shown.

6. Holasek, B.C., "Princeton Aircraft Design System (PADS): Wing and Tail Design Component", Princeton University Senior Independent Work Project Report, Jan 1983.

Detailed design of a three-dimensional wing or tail section can be accomplished using this program module. The wing geometry is specified by its planform and airfoil sections, allowing variations in sweep, aspect ratio, taper ratio, twist, dihedral, root chord, and tip chord. NACA 4-digit and 5-digit

airfoils are stored in the program, and the user can specify arbitrary airfoil sections by direct entry.

7. K.A. Farry and R.F. Stengel, "Distributed Processing and Fiber Optic Communications in Air Data Measurement", IEEE Transactions on Aerospace and Electronic Systems, Vol. AES-19, No. 3, May 1983, pp. 467 - 473.

   This paper describes the application of distributed processing, fiber optics, and hardware redundancy to collecting air data. Microprocessor-controlled instrumentation packages in each wingtip of Princeton's Variable-Response Research Aircraft (VRA) collect angle-of-attack and sideslip-angle data in digital form. After scaling, filtering, and calibrating the data, the wingtip processors send the data to the central processor, located in the VRA's fuselage, via fiber-optic links. The system design is presented, and results of a preliminary flight test are discussed. During this flight, over 2000 data transmissions occurred without error. The technology shows considerable promise for enhancing the reliability and performance of future flight control systems.

8. Bar-Gill, A., and Stengel, R.F., "Longitudinal Flying Qualities Criteria for Single-Pilot Instrument Flight Operations", SAE Paper No. 830761 for Business Aircraft Meeting & Exposition, Wichita, Apr 1983.

   Experiments to determine the flying qualities of more than a dozen dynamic configurations have been conducted using the variable-stability Avionics Research Aircraft. Particular attention was paid to variations in long-period longitudinal characteristics and their effects on the performance of simulated IFR flights from takeoff through landing. Over the range of values tested, lift slope had the greatest effect on pilot opinion, workload, and tracking error. Bounds for satisfactory flying qualities were found for three parameters: phugoid mode damping, stick force gradient (with respect to trim airspeed), and pitch/airspeed gradient.

FAILURE DETECTION AND IDENTIFICATION FOR A RECONFIGURABLE FLIGHT CONTROL SYSTEM

Francois Dallery
Princeton University
Princeton, New Jersey

OVERVIEW OF THE BASELINE CONFIGURATION

Failure detection and identification logic for a fault-tolerant longitudinal control system were investigated. Aircraft dynamics were based upon the cruise condition for a hypothetical transonic business jet transport configuration. The fault-tolerant control system consists of conventional control and estimation plus a new "outer loop" containing failure detection, identification, and reconfiguration (FDIR) logic. It is assumed that the additional logic has access to all measurements, as well as to the outputs of the control and estimation logic. The pilot also may command the FDIR logic to perform special tests.

- PARALLEL AND ANALYTICAL REDUNDANCY
- DETECTION AND IDENTIFICATION OF FAILURES IN:
  - STATE SENSORS
  - CONTROL EFFECTORS
  - CONTROL-EFFECTOR SENSORS
  - AIRFRAME CHARACTERISTICS
- TRANSONIC BUSINESS JET EXAMPLE

OVERVIEW OF THE BASELINE CONFIGURATION

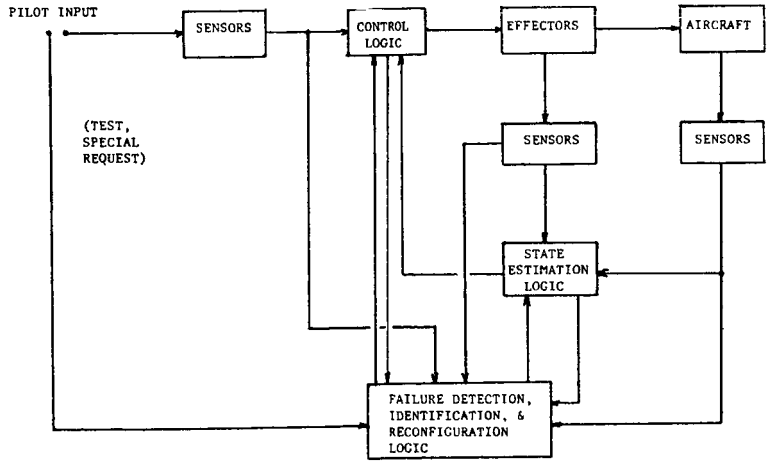

SIMULATION STRUCTURE

Simulation of the fault-tolerant control system was conducted using a general-purpose computer and the FORTRAN programming language. The simulation accounts for parallel redundancy in control system elements as well as analytical redundancy. The latter uses the mathematical relationships between dissimilar sensors to identify failures when it is suspected that one of two similar sensors has failed. It uses these same relationships to detect as well as identify failures when there is just one sensor of a kind. The logic distinguishes between failures of control effectors and failures of the sensors that measure control effector position. It also detects changes in aircraft dynamics, as might result from structural damage.

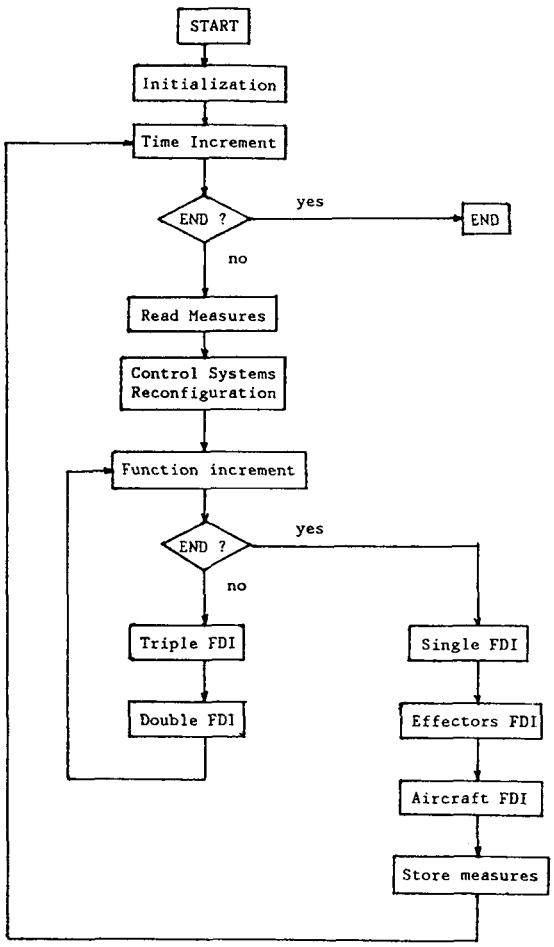

SINGLE-SENSOR FDI TREE

When there is no hardware redundancy remaining, failure detection and identification follows a tree structure, beginning with the simplest mathematical relationships between dissimilar sensors. For the most part, algebraic equations are used; however, it is necessary to use a Kalman filter to distinguish between angle-of-attack, manual-acceleration, and altitude sensor errors.

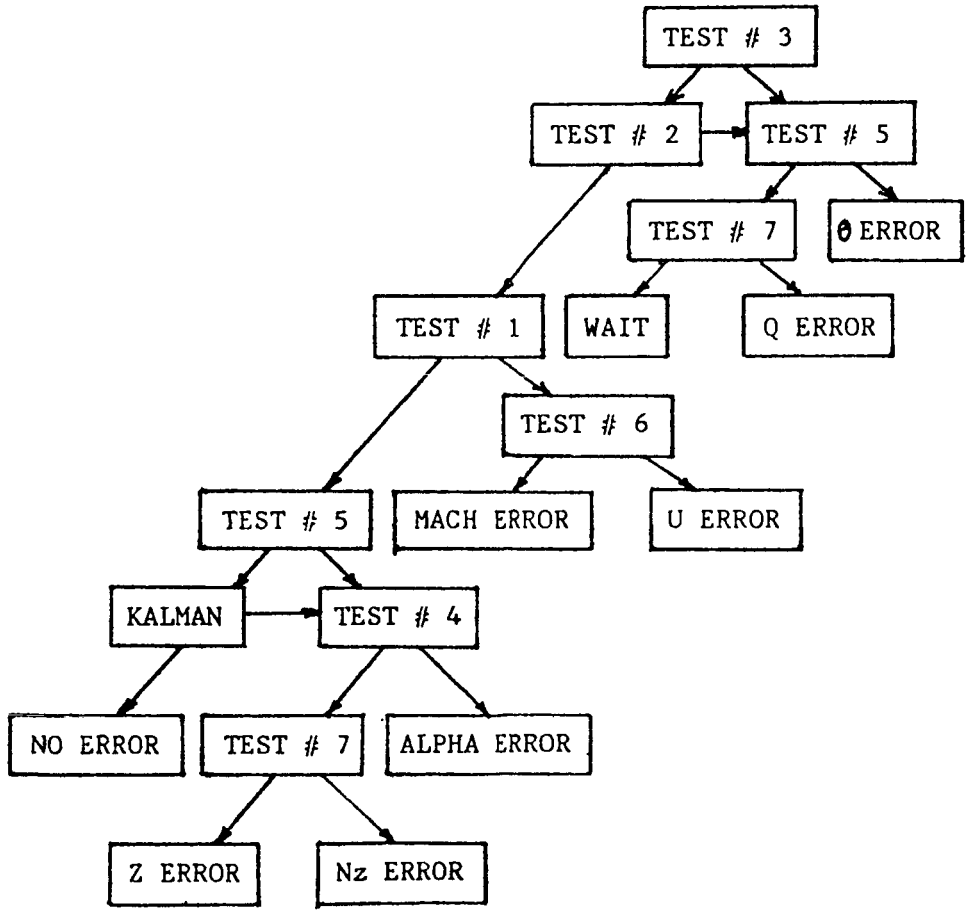

SINGLE-SENSOR STEP- AND RAMP-FAILURE

DETECTION TIMES

The threshold for failure detection was set just above the estimated 2.5-σ level. Step and ramp failures were simulated, with the results shown on the figure. The procedure generally was successful in detecting 5-σ step failures. It also could detect moderately steep (L/4) ramp-type failures; as the slope of the ramp decreased, detection times increased.

	Step 2.5 σ	Step 4. σ	Step 5. σ
M	No Detection	No Detection	Det. time = 6.60 sec.
q	No Detection	Det. time = 5.40 sec.	Not simulated
θ	No Detection	No Detection	Det. time = 21.60 sec.
α	No Detection	No Detection	Det. time = 31.80 sec.
Z	No Detection	No Detection	Det. time = 6.60 sec.
U	No Detection	No Detection	Det. time = 6.00 sec.
Nz	No Detection	No Detection	Det. time = 6.60 sec.

	Ramp L/4	Ramp L/7	Ramp L/10
M	Det. time = 15.00 sec.	Not Simulated	Det. time = 30.00 sec.
q	Det. time = 11.40 sec.	Not Simulated	Det. time = 24.60 sec.
θ	Det. time = 28.20 Sec.	Z Error detected	No detection in 60. sec.
α	Det. time - 28.20 sec.	Det. time = 34.20 sec.	Det. time = 60.0 sec.
Z	Det. time = 23.40 sec.	Det. time = 31.20 sec.	No detection in 60. sec.
U	Det. time = 15.00 sec.	Not Simulated	Det. time = 29.40 sec.
Nz	Det. time = 15.00 sec.	Not Simulated	Det. time = 29.40 sec.

EFFECTOR AND EFFECTOR-SENSOR

FAILURE DETECTION TIMES

Similar tests were made with errors in the control effectors and their sensors. These failures were detected quickly with 4-σ steps, and it was possible to distinguish readily between failures in the effectors and their associated sensors.

Additional results and conclusions are contained in the thesis by F. Dallery, "Failure Detection and Identification for a Reconfigurable Flight Control System," Princeton University Report No. MAE-1639T, Nov. 1983.

EFFECTOR FAILURES

	Step 2.5 σ	Step 4. σ	Ramp L/4.	Ramp L/10.
Elevator	No Detection	D.T = 4.80 sec.	D.T = 12.60 sec.	D.T = 24.00 sec.
Engine	No Detection	D.T = 5.40 sec.	D.T = 11.40 sec.	D.T = 24.00 sec.

FAILURES OF EFFECTOR SENSORS

	Step 2.5 σ	Step 4. σ	Ramp L/4.	Ramp L/10.
Elevator Sensor	No Detection	D.T = 4.80 sec.	D.t = 11.40 sec.	D.T = 24.00 sec.
Engine Sensor	No Detection	D.T = 4.80 sec.	D.T = 11.40 sec.	D.T = 24.00 sec.

AN APPLICATION OF ARTIFICIAL INTELLIGENCE THEORY TO RECONFIGURABLE FLIGHT CONTROL

David A. Handelman
Princeton University
Princeton, New Jersey

THE NEED FOR INTELLIGENT FLIGHT CONTROL

Many fatal aircraft accidents appear to be the result of a misuse of information, knowledge, or capability. For instance, a pilot depends on instruments for accurate aircraft status information. Inaccurate or partial information deprives the pilot of the resources necessary to safely operate the aircraft, and thus constitutes a misuse of information. Similarly, negligence or inexperience on the part of the pilot represents a misuse of knowledge. Finally, modern generic jet aircraft have highly redundant control effectors. As a result, it may be possible to counterbalance the effect of a failed primary control effector, such as an aileron, with a secondary control effector, such as a trailing-edge flap. If an aircraft is controllable following a failure, but through a lack of information, knowledge, or ability the pilot fails to control it, this represents a misuse of capability.

FATAL ACCIDENTS OF U.S. SCHEDULED AIR CARRIERS, 1961-1979

- REVERSE THRUST WARNING LIGHT MALFUNCTION
- LANDING GEAR WARNING LIGHT MALFUNCTION
- LOSS OF ELECTRICAL SYSTEM TO ATTITUDE INSTRUMENTS

- TURBULENCE, AIRFRAME FAILURE IN FLIGHT
- HYDRAULIC PRESSURE LOSS UNCORRECTED BY PILOT

- HYDRAULIC SYSTEM DEGRADATION
- RUDDER SUPPORT MATERIAL FAILURE
- RUDDER CONTROL SYSTEM MALFUNCTION
- FLIGHT CONTROL SYSTEM FAILURE
- FAILURE OF ENGINE PYLON

RESEARCH OBJECTIVES

The objective of this research is to use artificial intelligence techniques, along with statistical hypothesis testing and modern control theory, to help the pilot cope with the issues of information, knowledge, and capability in the event of a failure. We are developing an "intelligent" flight control system which utilizes knowledge of cause-and-effect relationships between all aircraft components. It will screen the information available to the pilot, supplement his knowledge, and most importantly, utilize the remaining flight capability of the aircraft following a failure. The list of failure types the control system will accommodate includes sensor failures, actuator failures, and structural failures.

PURPOSE

- TO INVESTIGATE THE POSSIBLE CONTRIBUTION OF ARTIFICIAL INTELLIGENCE TECHNIQUES TO AIRCRAFT FAILURE DETECTION, IDENTIFICATION, AND RECONFIGURATION (FDIR)

MOTIVATION

- MOST EXISTING FDIR SCHEMES CAN HANDLE ONLY A SUBSET OF ALL POSSIBLE AIRCRAFT FAILURES
- FEW EXISTING FDIR SCHEMES INCORPORATE HUMAN-LIKE COMMON SENSE OR KNOWLEDGE RELATING ALL AIRCRAFT COMPONENTS
- REDUNDANCY IN MODERN AIRCRAFT MAY PERMIT RECOVERY FROM SEVERE FAILURES

ASSUMPTIONS

In order to adapt to significant failure-induced changes in the configuration of the aircraft, the control system must have a variable structure. A fly-by-wire flight control system can be reconfigured by supplying new mathematical models and gains to the computer, thus a control system of this form is assumed. Note that the pilot flies the aircraft via the flight computer and has no direct link to the control surfaces. It is essential, therefore, that the flight computer have the model and gains corresponding to the actual aircraft configuration. Assuming that a failure will significantly change the configuration, it will be the job of the knowledge-based reconfigurable flight control system (KBRFCS) to replace the pre-failure model with the correct model.

BASIC FLY-BY-WIRE FLIGHT CONTROL SYSTEM

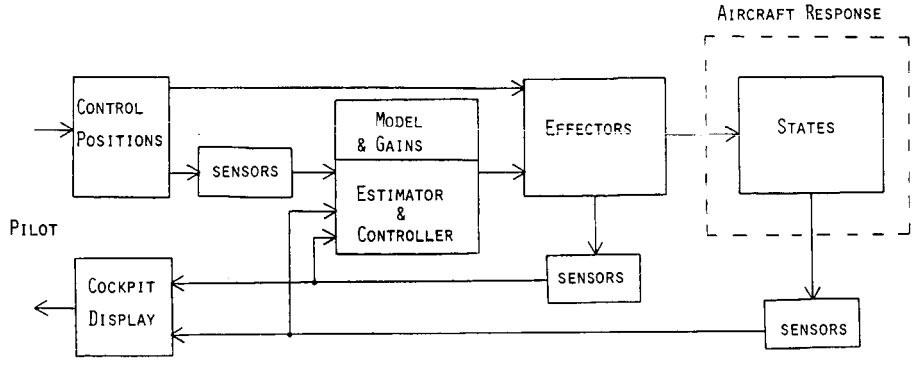

STATE - SPACE MODEL

$$\underline{x}(k+1) = \underline{\Phi}(k)\underline{x}(k) + \Gamma(k)\underline{u}(k) + \underline{G}(k) + \underline{w}(k)$$

$$\underline{y}(k) = H_x(k)\underline{x}(k) + H_u(k)\underline{u}(k) + \underline{B}(k) + \underline{v}(k)$$

$\underline{G}(k)$, $\underline{B}(k)$ = DETERMINISTIC BIASES

$\underline{w}(k)$, $\underline{v}(k)$ = INDEPENDENT, ZERO-MEAN GAUSSIAN WHITE NOISE PROCESSES

$$E\left[\underline{w}(k)\underline{w}(j)^T\right] = Q(k)\delta_{jk}$$

$$E\left[\underline{v}(k)\underline{v}(j)^T\right] = R(k)\delta_{jk}$$

A PROCEDURE FOR INTELLIGENT FAILURE MANAGEMENT

One method of dealing with the problem of failure detection, identification, and reconfiguration (FDIR) is the following. The KBRFCS supervises aircraft behavior until some abnormality occurs, at which time a failure alert is given. The system then allocates its resources to best serve the problem-solving process. This will be important if implementation requires a multi-microprocessor environment. Next, the system tries to diagnose exactly what has failed. Concurrently, immediate and temporary measures are taken to help reduce the effect of the failure during diagnosis. An example of such compensation would be the deflection of a flap to offset a sudden, unexplained roll. When the failure is identified, the best control configuration given the present circumstances is chosen and reconfiguration begins. Finally, the new control scheme is implemented.

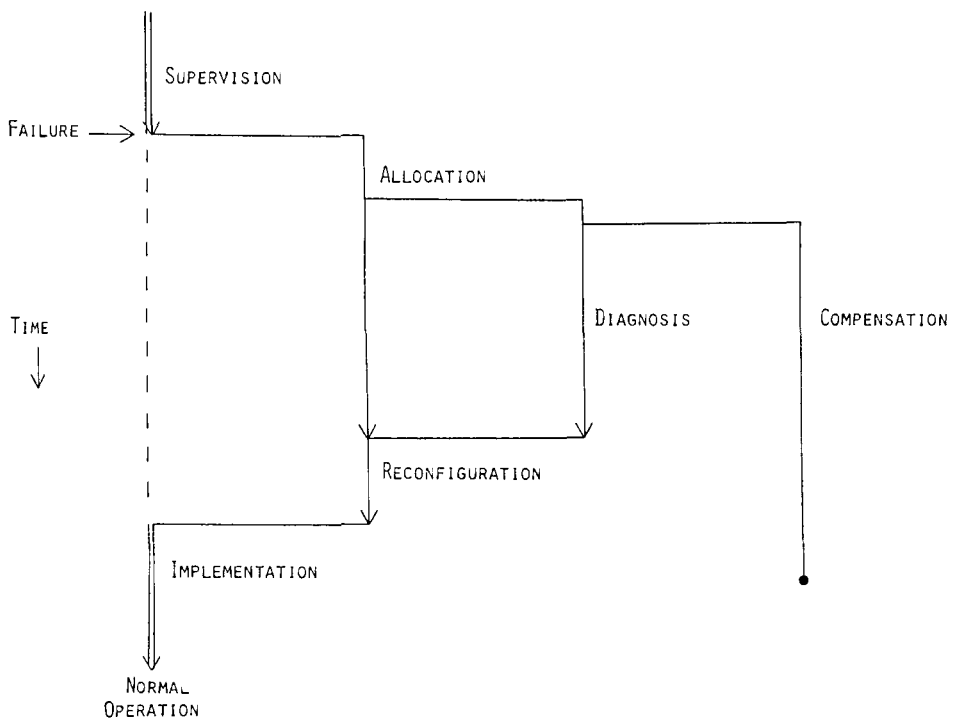

FAILURE DETECTION AND DIAGNOSIS PROBLEMS

The easiest way to detect and identify a sensor failure is to compare three sensors which measure the same quantity. Such a triplex system can be very expensive, however. In the less expensive duplex system a failure is easy to detect but hard to identify. Functional redundancy between unique sensors can be exploited to further reduce costs. For example, a rate gyro and an accelerometer can each provide pitch rate information; therefore, the signals can be compared to detect a failure in one of the two components. Although seemingly straightforward, these FDI techniques can run into problems. Consider a triplex system in which two of the sensors are powered from one electrical source and the third sensor from a different source. If the triplex FDI scheme identified a failure by singling out the one sensor which differed from the other two, a power failure to the first two sensors would be misconstrued as a failure of the third. This brings up the need for the incorporation of intelligence into the failure diagnosis process, an intelligence which will recognize when such "higher-order" relations among different elements of the aircraft exist.

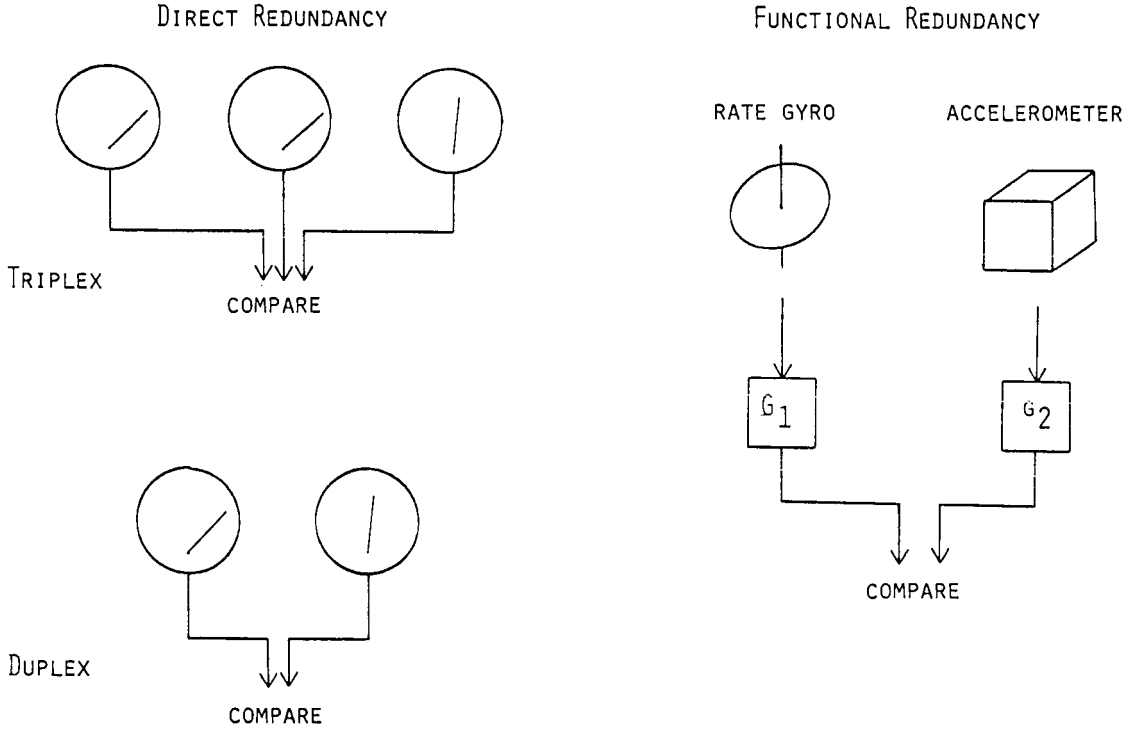

SOME EXISTING FAILURE DETECTION AND DIAGNOSIS SOLUTIONS

When the attempt is made to detect and diagnose all types of failures, not simply sensor failures, it is necessary to use all the analytical redundancy available. The generalized likelihood ratio (GLR) method and the multiple model (MM) method are two algorithms which use this redundancy to choose, from a finite set of alternatives, the mathematical model which best predicts the actual aircraft behavior. In FDI the set of alternatives would be the set of failures one hopes to detect and identify. The GLR method is well suited to failure detection, while the MM method is more effective at failure identification. Therefore, one way to accomplish FDIR would be to first detect a failure with the GLR, then run the MM algorithm to choose the proper model from the set of all possible failure models.

GENERALIZED LIKELIHOOD RATIO (GLR) METHOD

Basis

Different abrupt changes produce different effects on filter innovations

Advantages

- Likelihood calculations based on single nominal Kalman Filter
- With magnitude of failure known, simplified GLR (SGLR) results in very low computational load
- Effectively detects abrupt changes

Disadvantages

- Accommodates additive effects on single nominal model only

MULTIPLE MODEL (MM) METHOD

Operation

- Observe u(k) and y(k)
- Choose most likely model from finite set of hypotheses
- Recursive probability formula from Bayes' Rule

Advantages

- Allows parametric as well as additive changes
- Compares models of different order
- Robust to non-Gaussian statistics

Disadvantages

- High computational burden
- Bank of Kalman Filters
- Switch detection requires growing number of filters
- Slow response to model switches

AN ALTERNATE SOLUTION

The KBRFCS will be expected to handle many types of failures. Each failure will change the aircraft configuration in a unique way and will therefore have a unique model associated with it. If the previously mentioned FDIR scheme is employed, the MM algorithm will be required to choose from among thousands of models. Although this may be a theoretically feasible solution, it will require an immense amount of computing power. Our goals include eventual implementation and flight testing of the control system, and computer resources must be kept to a minimum. If there was a way to let the MM algorithm test only those models corresponding to failures which are most likely under the circumstances, the required computer speed could be drastically reduced. In the KBRFCS, this important diagnostic tool takes the form of an expert system.

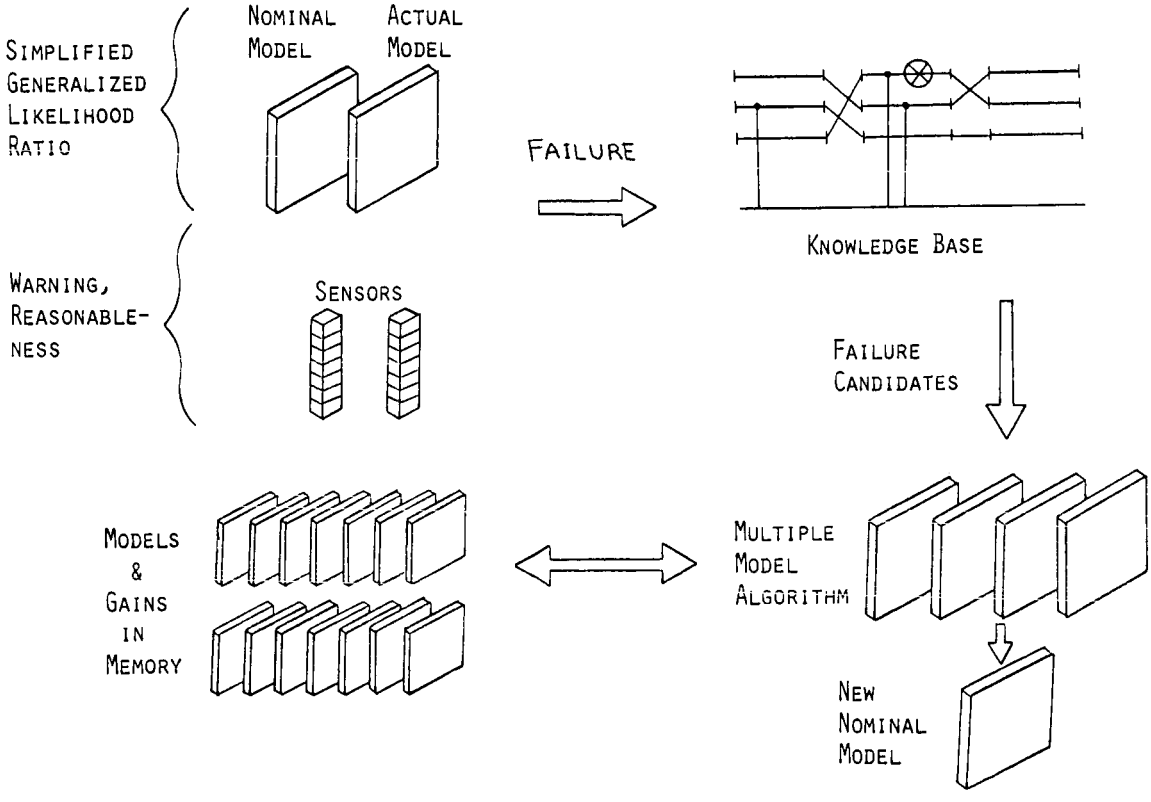

THE EXPERT SYSTEM

The job of the expert system is to narrow down to a reasonable number the list of possible failures to be tested by the MM algorithm. When a sensor value goes beyond a prespecified warning level, or if it jumps too quickly, or if a state or observation bias jump is picked up by the GLR, a failure is detected and this information is passed on to the expert system. With knowledge of the cause-and-effect relationships among all aircraft components and common-sense failure diagnosis rules, the expert system decides which failures are most likely to have occurred.

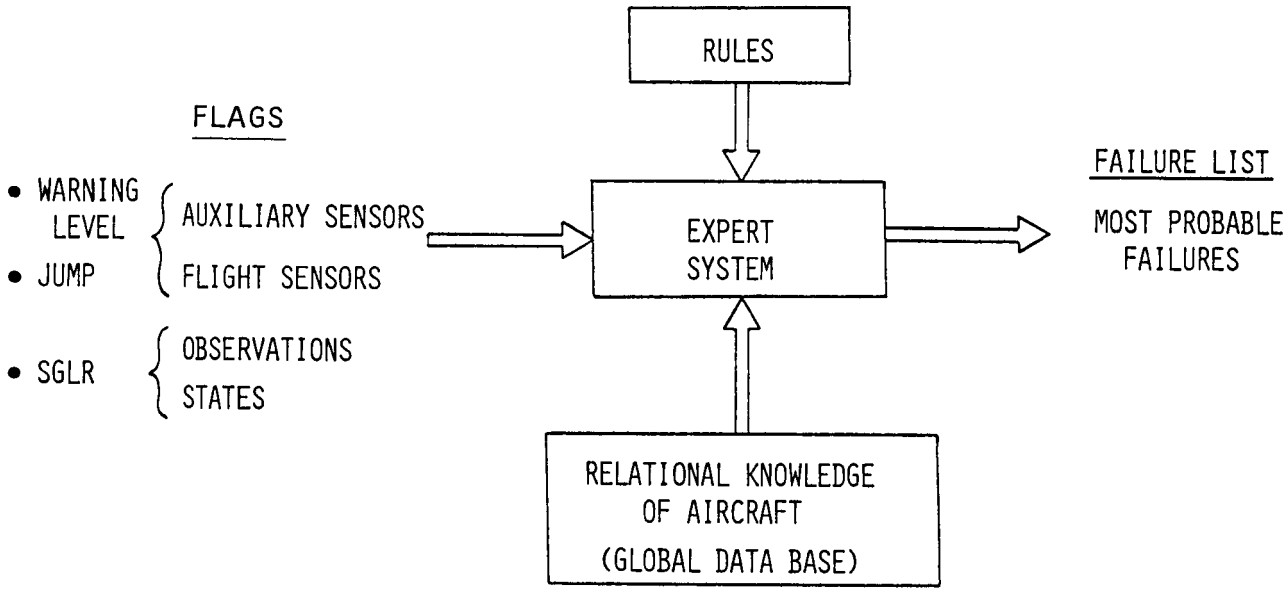

THE GLOBAL DATA BASE AND THE RULES

The aircraft relational knowledge is contained in the global data base. The rules combine this knowledge with heuristic, common-sense reasoning to diagnose a failure. The following example illustrates the type of rules the expert system contains.

Rule #1 — If a sensor (such as an aileron position sensor) has exceeded its expected value and that sensor senses an effector (such as an aileron) and no states (including roll rate) have exceeded their expected values then - a sensor failure is likely and an electrical support (for that sensor) failure is likely.

Rule #2 — If a sensor has exceeded its expected value and that sensor senses an effector and that effector strongly effects a state which has exceeded its expected value
then - an effector failure is likely.

These rules show how the expert system can distinguish between a failed effector which is sensed and a failed sensor.

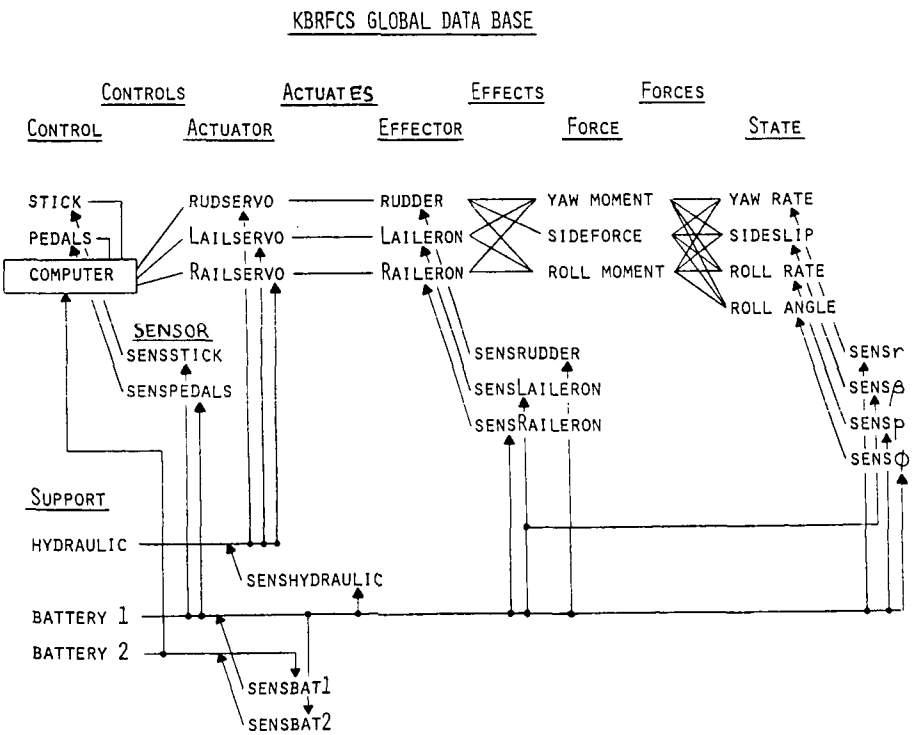

Although the expert system contains many rules, only a small number of them will be pertinent to a given failure at a given point in the diagnostic process. For example, if a failure is detected and no state bias jumps were observed by the GLR test, the expert system should not waste time testing rules which depend on the existence of a state bias jump in order to be true. The "rule interpreters" provide the control structure needed to select the appropriate rules to be tested. With the expert system complete, the KBRFCS becomes an intelligent and valuable mechanism capable of accommodating failures that a pilot may not be able to handle alone.

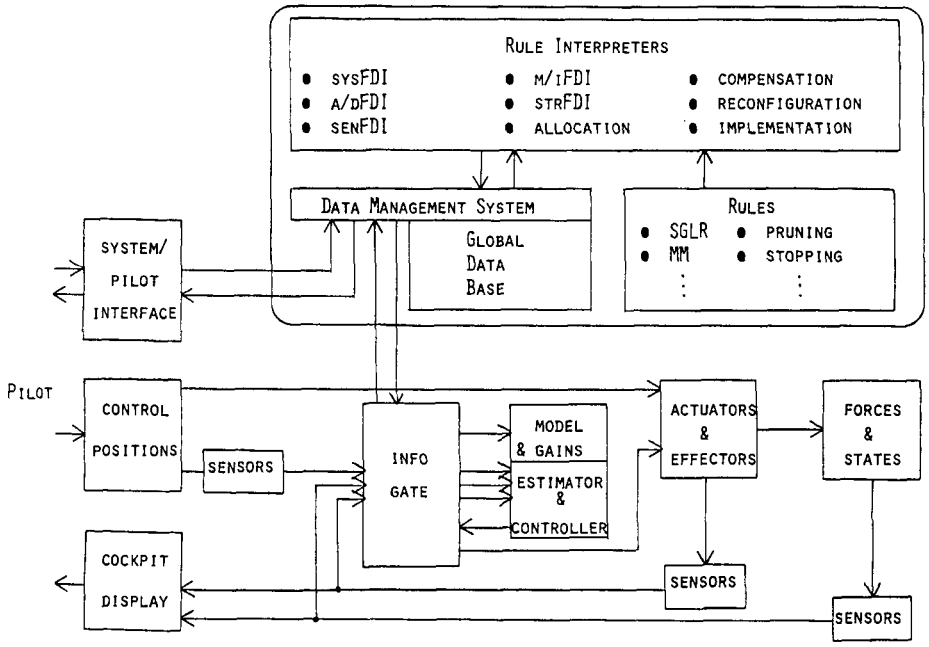

RESEARCH WORK SCHEDULE

- THEORETICAL DEVELOPMENT
- NOMINAL MODEL SELECTION
- FAILURE SET GENERATION
- GAIN CALCULATION
- KNOWLEDGE GENERATION THROUGH GLR, SGLR, AND MM TESTING
- GENERAL RULE DEVELOPMENT
- GLOBAL DATA BASE DEVELOPMENT
- SPECIFIC RULE DEVELOPMENT
- RULE INTERPRETER DEVELOPMENT
- MULTI-MICROPROCESSOR SIMULATION

N87-18531

DEVELOPMENT OF CONTROL STRATEGIES FOR SAFE MICROBURST PENETRATION:

A PROGRESS REPORT

Mark L. Psiaki
Mechanical and Aerospace Engineering Department
Princeton University
Princeton, New Jersey

REVIEW OF WORK DONE PRIOR TO SEPTEMBER 1983

A microburst, a downburst of horizontal extent less than 3 miles, consists of a vertically descending column of air that spreads out horizontally as it hits the ground. A penetrating aircraft first encounters a headwind which causes a pitch-up and a rise above the flight path. Then it experiences a shear of the headwind to a tailwind along with a downdraft, both of which cause it to fall below the glide path.

A nonlinear simulation of the longitudinal equations of motion of a Jet Transport aircraft that includes wind inputs was used to study the transient response to a microburst. These were compared to plots of the aircraft's frequency response to wind inputs as generated from a linearized model.

Various loop closures were studied using root locus analysis and the above-mentioned frequency response and transient response plots. Feedback of air-relative specific energy rate to the throttle yielded improvements in frequency response, but not in transient response to microburst due to throttle saturation. Feedback of $\bar{q}\alpha$ (the normal load factor) or airspeed (with wrong sign) to the elevator yielded improvements both in frequency response and in transient response to microburst.

- MICROBURST WIND SHEAR HAZARD
- NONLINEAR LONGITUDINAL SIMULATION
- BODE PLOTS OF FREQUENCY RESPONSE TO WIND INPUTS
- EFFECTS OF VARIOUS LOOP CLOSURES
  - → ROOT LOCI
  - → FREQUENCY RESPONSE
  - → NONLINEAR TRANSIENT RESPONSE

WORK DONE SINCE SEPTEMBER 1983

A single-engine, propeller-driven, general-aviation model was incorporated into the nonlinear simulation and into the linear analysis of root loci and frequency response. Full-scale wind tunnel data provided its aerodynamic model, and the thrust model included the airspeed dependent effects of power and propeller efficiency.

Also, the parameters of the Jet Transport model were changed to correspond more closely to a Boeing 727.

In order to study their effects on steady-state response to vertical wind inputs, altitude and total specific energy (air-relative and inertial) feedback capabilities were added to the nonlinear and linear models.

Multiloop systems design goals were defined. Attempts were made to develop controllers which achieved these goals.

- INCORPORATION OF GENERAL AVIATION (GA) MODEL
- IMPROVEMENT OF JET TRANSPORT (JT) MODEL
- CONSIDERATION OF ALTITUDE AND TOTAL ENERGY TYPE FEEDBACK
- ATTEMPT AT MULTILOOP CONTROLLER DESIGN

EFFECTS OF ALTITUDE/ENERGY FEEDBACK

In the literature one finds the altitude error being fed back to the elevator to attenuate response to vertical wind inputs. For the purposes of this study, this does not work well due to stability limitations imposed by the non-minimum phase relation between the elevator and the altitude and by the effects of being on the backside of the power curve.

Feedback of total air-relative specific energy to the throttle satisfactorily stabilizes the neutrally stable altitude mode. Addition of energy rate feedback to the loop provides further stability improvements and improves transient response to microbursts by adding lead information.

- ALTITUDE-TO-ELEVATOR LOOP
- TOTAL AIR-RELATIVE SPECIFIC ENERGY-TO-THROTTLE LOOP
- TOTAL AIR-RELATIVE SPECIFIC ENERGY-PLUS-TOTAL AIR-RELATIVE SPECIFIC ENERGY RATE-TO-THROTTLE LOOP

ROOT LOCUS, PHUGOID PORTION, H_a-PLUS-$\dot{H}_a$-TO-δT FEEDBACK

Although the rigid-body longitudinal motion of the aircraft and the engine dynamics and altitude feedback yield a sixth-order system, the root locus for feedback of specific energy to throttle resembles that of a second-order system. This is because total specific energy varies little with phugoid or short period oscillations. By adding specific energy rate feedback such that the new zero is just to the left of the engine dynamics pole, the root locus resembles that of a first-order system and desirable stability characteristics can be achieved.

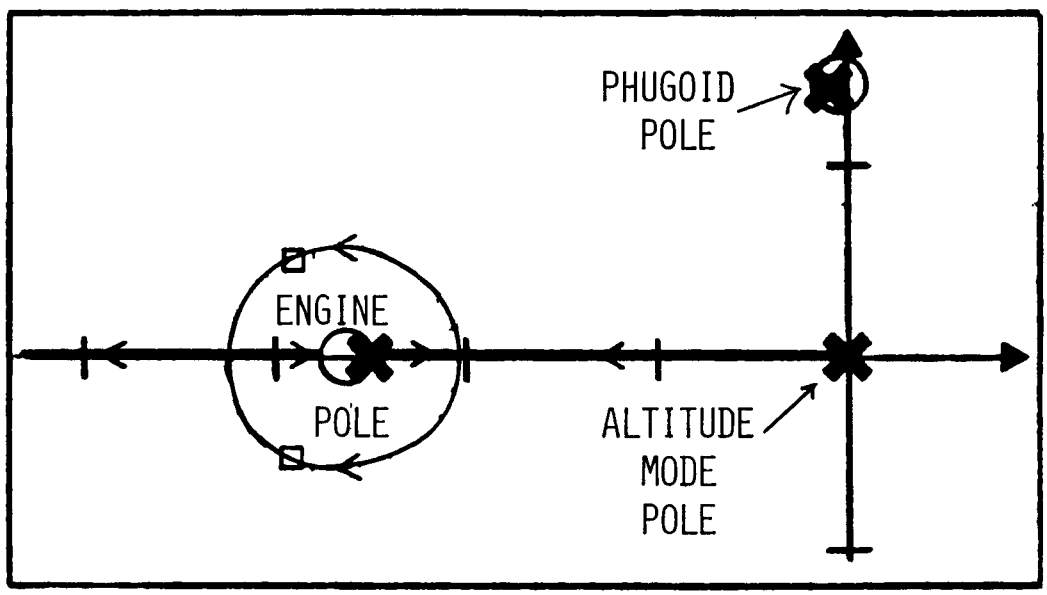

MULTI-LOOP CONTROLLER DESIGN

Examination of open-loop frequency response and transient response to microbursts yielded three main results.

1. Open-loop aircraft response to the head/tail wind shear of a microburst is extreme when the characteristic frequency of the microburst is near that of the phugoid's natural frequency.

2. Open-loop response to the head/tail wind shear is still unacceptably high for excitation frequencies below that of the phugoid.

3. Response to the down draft resembles that of an integrator responding to a finite-width impulse and can be unacceptably high for the open-loop case and typical microbursts.

The stated design criteria were developed with alleviation of these effects in mind.

The first of the two control laws attempts to satisfy the first two design criteria, while the second control law does a reasonable job of satisfying all three criteria, provided the aircraft does not stall.

- DEVELOPMENT OF WIND SHEAR ATTENUATION DESIGN CRITERIA
  - → INCREASE IN PHUGOID DAMPING
  - → ELIMINATION OF INTEGRATION RESPONSE TO VERTICAL WIND INPUT
  - → REDUCTION OF LOW FREQUENCY RESPONSE TO HORIZONTAL WIND INPUTS

- MULTI-LOOP-CONTROLLERS
  - → θ_i-TO-δE AND H_a-TO-δT
  - → $\bar{q}\alpha$-PLUS-γ_i-TO-δE AND H_a-PLUS-$\dot{H}_a$-TO-δT

ALTITUDE FREQUENCY RESPONSE TO HORIZONTAL AND VERTICAL WIND INPUTS WITH $\bar{q}\alpha$-PLUS-γ_i-FEEDBACK TO-δE AND H_a-PLUS-$\dot{H}_a$-FEEDBACK TO δT

The effects of two multi-loop control laws on frequency response, both to vertical and to horizontal wind inputs, are shown here in comparison with the open-loop case. The feedback of H_a-to-δT changes the order of the system, stabilizing the altitude mode pole and raising the low-frequency slopes of both plots by 20 dB/decade. Addition of an $\dot{H}_a$-to-δT loop further lowers the low-frequency response to horizontal wind input. Feedback of θ_i-to-δE or $\bar{q}\alpha$-plus-γ_i-to-δE eliminates the resonant peak at the phugoid natural frequency. Feedback of $\bar{q}\alpha$-plus-γ_i-to-δE lowers the natural frequency of the phugoid, thus lowering the peak response to horizontal wind inputs, but this loop also raises the low-frequency response to vertical wind inputs because of the effects of being on the backside of the power curve.

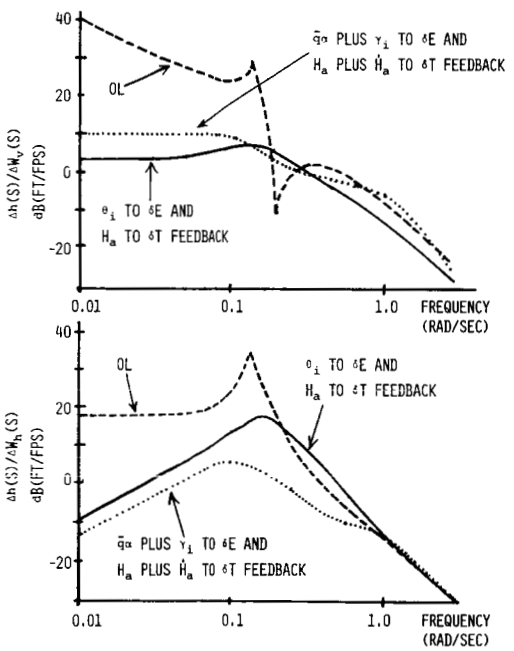

TRANSIENT RESPONSE TO MICROBURST WITH $\bar{q}\alpha$-PLUS-γ_i-TO-δE FEEDBACK

AND H_a-PLUS-$\dot{H}_a$-TO-δE FEEDBACK

These simulation results of approach trajectories through a microburst tuned to the jet transport phugoid show that the control law which satisfied all three design criteria also yielded the best trajectory tracking performance in transient response to a microburst. Neither control law yielded as low a transient response as was predicted by the frequency response plots because throttle saturation occurred in both cases.

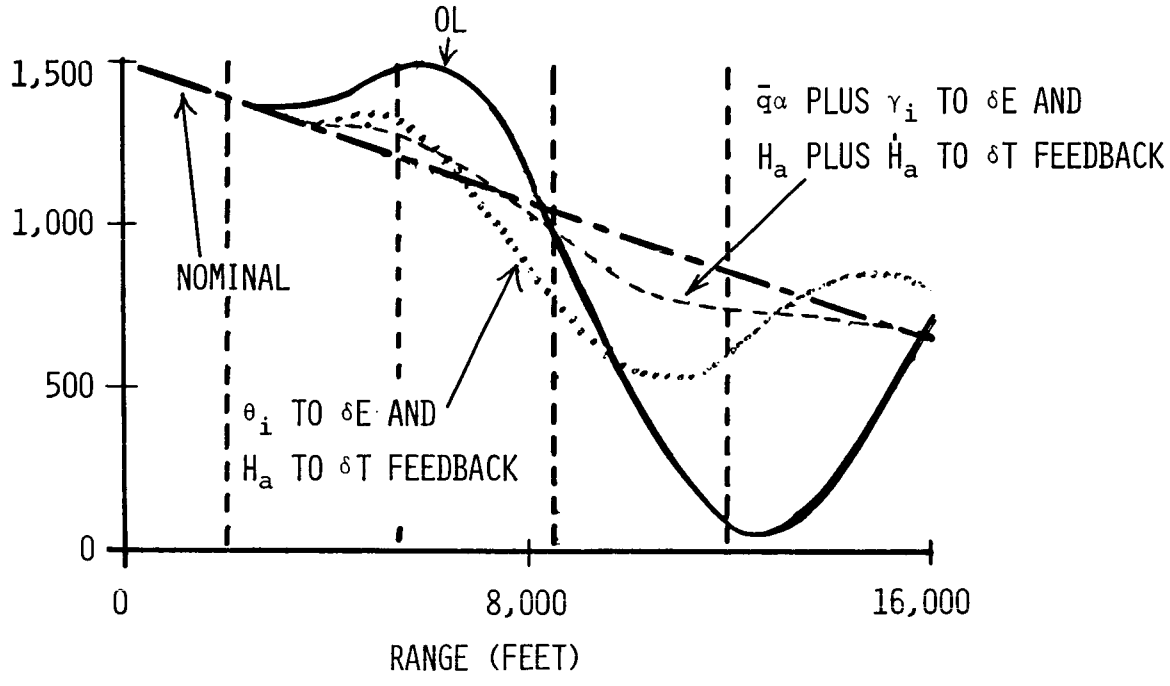

COMPARISON OF OPEN-LOOP AND CLOSED-LOOP TRANSIENT

RESPONSE TO MICROBURST FOR TWO AIRCRAFT

These simulation results of approach trajectories through a microburst compare both open-loop and closed-loop curves for both the general-aviation and jet transport aircraft. The general-aviation response to the head/tail wind shear is lower in both the open-loop and closed-loop cases because this microburst is tuned to the jet transport's phugoid, and therefore forces the general-aviation aircraft at a frequency far below its phugoid natural frequency. The general-aviation response to the downdraft, however, is more severe because of its lower wing loading and its lower nominal velocity (longer time in the downdraft). In the closed-loop case, this causes the general-aviation aircraft to stall because of the $\bar{q}\alpha$-plus-γ_i-to-δE feedback loop.

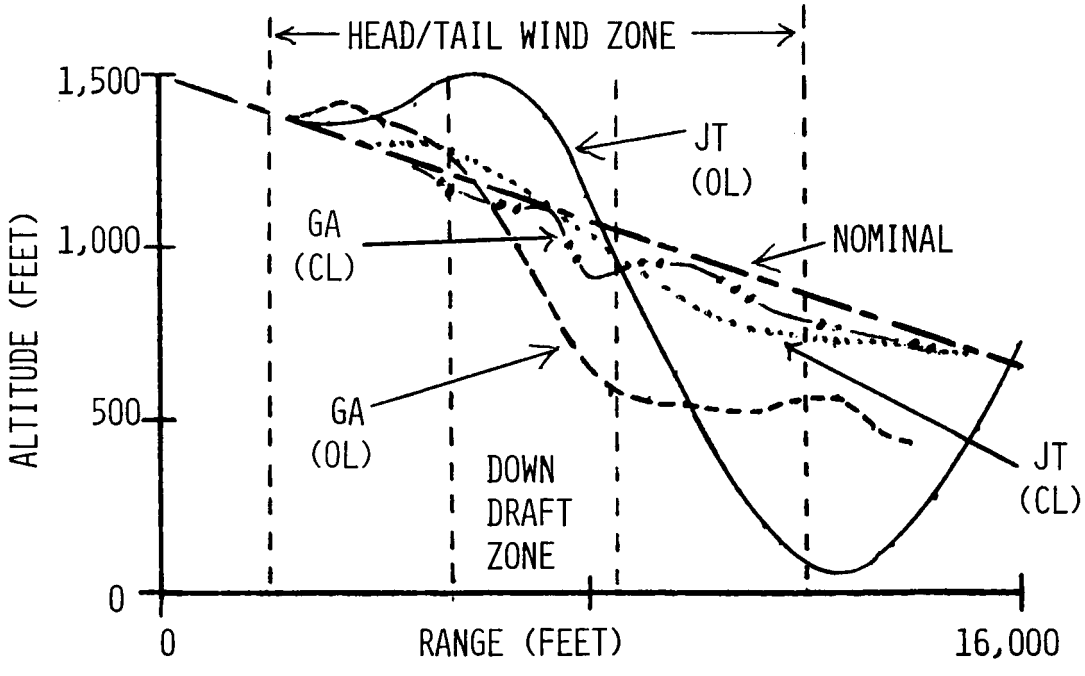

CONCLUSIONS

Although exact prediction of transient response using frequency response plots is not possible due to control saturation and the steady-state nature of the plots, frequency response to wind shear is a useful tool for control law evaluation. Because throttle saturation and aircraft stall limits are significant factors in determining microburst penetration capability, nonlinear simulation of microburst encounter is essential to the evaluation of control laws. The best multi-loop control law tested to date incorporated both energy management relative to the air mass via throttle and a pitch-up response to decreasing airspeed.

- CORRELATION BETWEEN BODE FREQUENCY RESPONSE PLOTS AND SIMULATION RESULTS
- SIGNIFICANCE OF THROTTLE SATURATION AND AIRCRAFT STALL NONLINEARITIES TO PERFORMANCE LIMITS
- NEED FOR NONLINEAR SIMULATIONS
- IMPORTANCE OF ENERGY MANAGEMENT RELATIVE TO THE AIR-MASS FOR TRAJECTORY TRACKING
- BENEFIT OF PITCH-UP RESPONSE TO DECREASING AIRSPEED

PLANNED FUTURE WORK

The current microburst model has only the basic features of the headwind, downdraft, and tailwind sequence. Better models, based upon meteorological data, are becoming available and should be used to evaluate final designs.

There remains some question as to the validity of the point-aircraft, quasi-steady aerodynamics model which is used by most researchers in this field. Again, a thorough validation of the model must be made before any final conclusions are reached.

Wind shear estimation and cancellation of wind shear-induced forces and moments in a feed-forward control law are possibly useful approaches to safer microburst encounter.

As yet, the best possible performance of an aircraft during microburst encounter has not been determined. This calculation is a lengthy, but straightforward application of nonlinear optimal control theory. It will demonstrate the limits of the performance envelope and will possibly lead to the development of previously unknown techniques for safe microburst penetration. Also stochastic optimal control techniques may be useful to the development of practical control laws which attenuate the aircraft response to a microburst.

- IMPROVE MICROBURST MODEL
- CHECK VALIDITY OF QUASI-STEADY, POINT AERODYNAMIC MODEL
- STUDY FEED-FORWARD CONTROL
    1. WIND SHEAR ESTIMATION
    2. GENERALIZED FORCE CANCELLATION
- APPLY OPTIMAL CONTROL THEORY
    1. TRUE OPTIMUM - REQUIRES KNOWLEDGE OF FUTURE DISTURBANCE
    2. PRACTICAL OPTIMUM - DISTURBANCE TREATED AS RANDOM

Standard Bibliographic Page

1. Report No.	2. Government Accession No.	3. Recipient's Catalog No.
NASA CP-2451		

4. Title and Subtitle	5. Report Date
Joint University Program for Air Transportation Research - 1983	March 1987
	6. Performing Organization Code: 505-66-01-07
7. Author(s)	8. Performing Organization Report No.
Frederick R. Morrell, Compiler	L-16254
9. Performing Organization Name and Address	10. Work Unit No.
NASA Langley Research Center Hampton, VA 23665-5225	11. Contract or Grant No.
12. Sponsoring Agency Name and Address	13. Type of Report and Period Covered: Conference Publication
National Aeronautics and Space Administration Washington, DC 20546-0001	14. Sponsoring Agency Code

15. Supplementary Notes

16. Abstract

This report summarizes the research conducted during 1983 under the NASA/FAA sponsored Joint University Program for Air Transportation Research. The material was presented at a conference held at the Federal Aviation Administration Technical Center, Atlantic City, New Jersey, December 16, 1983. The Joint University Program is a coordinated set of three grants sponsored by NASA Langley Research Center and the Federal Aviation Administration, one each with the Massachusetts Institute of Technology, Ohio University, and Princeton University. Completed works, status reports, and bibliographies are presented for research topics, which include navigation, guidance, control, and display concepts. An overview of the year's activities for each of the universities is also presented.

17. Key Words (Suggested by Authors(s))	18. Distribution Statement
Air transportation Avionics Low-frequency terrestrial navigation Aircraft guidance navigation and control	Unclassified - Unlimited Subject Category 01

19. Security Classif.(of this report)	20. Security Classif.(of this page)	21. No. of Pages	22. Price
Unclassified	Unclassified	86	A05

For sale by the National Technical Information Service, Springfield, Virginia 22161

NASA-Langley, 1987